ELSEVIER

Prog. Polym. Sci. 25 (2000) 677–710

PROGRESS IN
POLYMER SCIENCE

Polymer brushes: surface-immobilized macromolecules

B. Zhao, W.J. Brittain*

Department of Polymer Science, The University of Akron, Akron, OH 44325-3909, USA

Received 25 February 2000; revised 17 April 2000; accepted 17 April 2000

Abstract

This article reviews recent literature on polymer brushes with an emphasis on linear polymer brushes attached to solid substrate surfaces. The following topics are included: (i) theoretical and experimental studies of homopolymer brush structure; (ii) theoretical investigations of diblock copolymer brushes; (iii) preparation of homopolymer brushes by physisorption, "grafting to" and "grafting from" methods; (iv) synthesis of diblock copolymer brushes; and (v) fabrication of patterned polymer brushes.

Keywords: Polymer brush; Tethered polymer; Self-assembled monolayers; Surface-immobilized initiators

Contents

* Corresponding author.
E-mail address: brittain@polymer.uakron.edu (W.J. Brittain).

0079-6700/00/$ - see front matter
PII: S0079-6700(00)00012-5

1. Introduction to polymer brushes

Polymer brushes refer to an assembly of polymer chains which are tethered by one end to a surface or an interface [1–3]. Tethering is sufficiently dense that the polymer chains are crowded and forced to stretch away from the surface or interface to avoid overlapping, sometimes much farther than the typical unstretched size of a chain. These stretched configurations are found under equilibrium conditions; neither a confining geometry or an external field is required. This situation, in which polymer chains stretch along the direction normal to the grafting surface, is quite different from the typical behavior of flexible polymer chains in solution where chains adopt a random-walk configuration. A series of discoveries show that the deformation of densely tethered chains affects many aspects of their behavior and results in many novel properties of polymer brushes [2].

Polymer brushes are a central model for many practical polymer systems such as polymer micelles; block copolymers at fluid–fluid interfaces (e.g. microemulsions and vesicles), grafted polymers on a solid surface, adsorbed diblock copolymers and graft copolymers at fluid–fluid interfaces. All of these systems, illustrated in Fig. 1, have a common feature: the polymer chains exhibit deformed configurations. Solvent can be either present or absent in polymer brushes. In the presence of a good solvent, the polymer chains try to avoid contact with each other to maximize contact with solvent molecules. With solvent absent (melt conditions) polymer chains must stretch away from the interface to avoid overfilling incompressible space.

The interface to which polymer chains are tethered in the polymer brushes may be a solid substrate surface or an interface between two liquids, between a liquid and air, or between melts or solutions of homopolymers. Tethering of polymer chains on the surface or interface can be reversible or irreversible. For solid surfaces, the polymer chains can be chemically bonded to the substrate or may be just adsorbed onto the surface. Physisorption on a solid surface is usually achieved by block copolymers with one block interacting strongly with the substrate and another block interacting weakly. For interfaces between fluids, the attachment may be achieved by similar adsorption mechanisms in which one part of the chain prefers one medium and the rest of the chain prefers the other.

Polymer brushes (or tethered polymers) attracted attention in 1950s when it was found that grafting polymer molecules to colloidal particles was a very effective way to prevent flocculation [4–9]. In other words, one can attach polymer chains which prefer the suspension solvent to the colloidal particle surface; the brushes of two approaching particles resist overlapping and colloidal stabilization is achieved. The repulsive force between brushes arises ultimately from the high osmotic pressure inside the brushes. Subsequently it was found that polymer brushes can be useful in other applications such as new adhesive materials [10,11], protein-resistant biosurfaces [12], chromotographic devices [13], lubricants [14], polymer surfactants [1] and polymer compatibilizers [1]. Tethered polymers which possess low critical solution temperature (LCST) properties exhibit different wetting properties above and below LCST temperature [15]. A very promising field that has been extensively investigated is using polymer

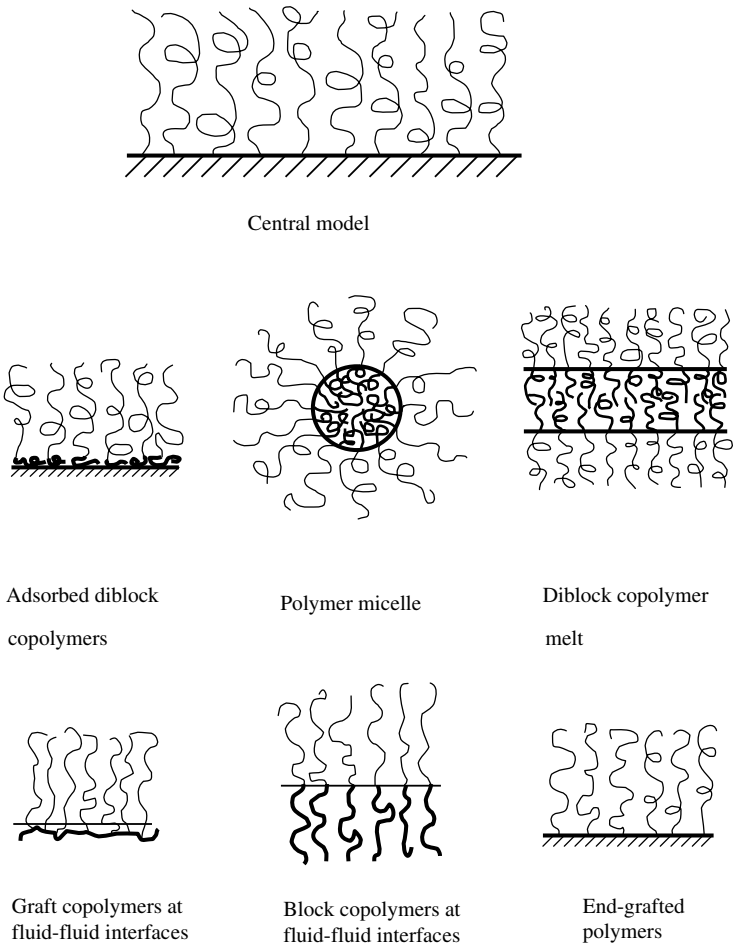

Fig. 1. Examples of polymer systems comprising polymer brushes.

brushes as chemical gates. Ito et al. [16–18]. have reported pH sensitive, photosensitive, oxidoreduction sensitive polymer brushes covalently tethered on porous membranes, which are used to regulate the liquid flowing rate through porous membranes. Suter and coworkers [19,20] have prepared polystyrene brushes on high surface area mica for the fabrication of organic–inorganic hybrids. Cation-bearing peroxide free-radical initiators were attached to mica surfaces via ion exchange and used to polymerize styrene. This process is important in the field of nanocomposites. Patterned thin organic films could be useful in microelectrics [21], cell growth control [22,23], biomimetic material fabrication [24], micro-reaction vessel and drug delivery [25].

This review will be restricted to linear polymer brushes on solid substrate surfaces. In terms of polymer chemical compositions, polymer brushes tethered on a solid substrate surface can be divided into homopolymer brushes, mixed homopolymer brushes, random copolymer brushes and block copolymer brushes. Homopolymer brushes refer to an assembly of tethered polymer chains consisting of one type of repeat unit. Mixed homopolymer brushes are composed of two or more types of homopolymer

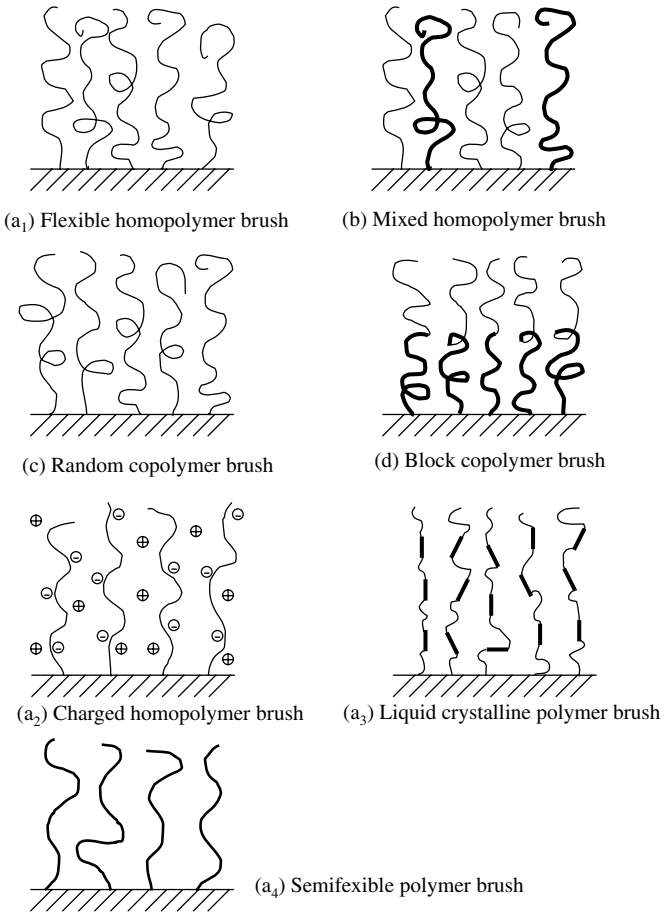

Fig. 2. Classification of linear polymer brushes, (a_1–a_4) homopolymer brushes; (b) mixed homopolymer brush; (c) random copolymer brush; (d) block copolymer brush.

chains [26]. Random copolymer brushes refer to an assembly of tethered polymer chains consisting of two different repeat units which are randomly distributed along the polymer chain [27]. Block copolymer brushes refer to an assembly of tethered polymer chains consisting of two or more homopolymer chains covalently connected to each other at one end [28]. Homopolymer brushes can be further divided into neutral polymer brushes and charged polymer brushes. They may also be classified in terms of rigidity of the polymer chain and would include flexible polymer brushes, semiflexible polymer brushes and liquid crystalline polymer brushes. These different polymer brushes are illustrated in Fig. 2.

The study of polymer brushes extends into many fields, including physics, chemistry, material science and engineering. During the last two decades many scientists have investigated the behavior of the tethered layers using experimental and theoretical methodologies. This review is organized as follows. Theoretical and experimental studies of homopolymer brushes will be briefly discussed in Section 2. Theoretical consideration of the behavior of the tethered diblock copolymer brushes will be summarized

in Section 3. Preparation of homopolymer brushes by physisorption, "grafting to" and "grafting from" approaches will be reviewed in Section 4. Synthesis of tethered diblock copolymer brushes and patterned polymer brushes will be discussed in Sections 5 and 6.

2. Theoretical and experimental studies of homopolymer brushes

2.1. Theoretical studies of flexible homopolymer brushes

Alexander [29] was one of the first scientists who noted the distinctive properties of polymer brushes through theoretical analysis concerning the end-adsorption of terminally functionalized polymers on a flat surface. Further elaboration by de Gennes [30,31] and by Cantor [32] stressed the utility of tethered chains to the description of self-assembled block copolymers. The internal structure of polymer brushes was illustrated by numerical and analytical self-consistent field (SCF) calculations, and by computer simulations.

The configurational space of the polymer chains is limited by the presence of an interface in polymer brushes. The deformation of densely tethered polymer chains reflects a balance between interaction and elastic free energies. Dense tethering of polymer chains on an interface enforces a strong overlap among the undeformed coils, increases the monomer–monomer unit contacts and the corresponding interaction energy. The polymer chains are forced to stretch away along the direction normal to the grafting sites, thereby lowering the monomer concentration in the layer and increasing the layer thickness, L. Stretching lowers the interaction energy per chain, F_{int}, at the price of a high elastic free energy, F_{el}. The interplay of these two terms determines the equilibrium thickness of the layer.

It is easy to use the Alexander model to make this argument clearer [2,29]. The Alexander model considers a flat, nonadsorbing surface to which monodisperse polymer chains are tethered. The polymer chains consist of N statistical segments of diameter a, the average distance between the tethering point is d, which is much smaller than the radius of gyration of a free, undeformed chain. The free energy per chain includes two terms:

$$F = F_{\text{int}} + F_{\text{el}} \tag{2.1}$$

F_{int} refers to the interaction energy between two statistical segments and F_{el} refers to the elastic free energy. Two assumptions are made to enable simple expressions for these two terms. The first one is that the depth profile of statistical segments is step-like. The concentration of statistical segments is a constant within brushes, $\varphi = Na^3/d^2L$. The second is that all free ends of tethered polymer chains are located in the single plane at a distance L from the tethering surface.

The "Flory approximation" [33] is used to obtain an explicit expression for free energy. This argument estimates the reduction in configurational entropy from results for an ideal random walk chain constrained to travel a distance L from the grafting surface to the outer edge of the polymer brush. The corresponding free energy per chain can be expressed in the following equation:

$$F/\text{k}T \approx \nu\varphi^2 d^2 L/a^3 + L^2/R_0^2 \tag{2.2}$$

where v is a dimensionless excluded volume parameter and R_0 is the radius of an unperturbed, ideal coil. The first term represents the interaction energy between statistical segments and the second represents the elasticity of Gaussian chains. A "scaling argument" approach gives a similar result. The equilibrium

Table 1
The relationship between the dimensions of polymer chains and N under various conditions

	Tethered polymer chain	Free polymer chain
Good solvent	$L/a \approx N(a/d)^{2/3}$	$R_g \sim N^{3/5}$
Theta solvent	$L/a \approx N(a/d)$	$R_g \sim N^{1/2}$
Bulk state	$L \sim N^{2/3}$	$R_g \sim N^{1/2}$

thickness is obtained by minimization of F with respect to L and is shown in the following equation:

$$L/a \approx N(a/d)^{2/3} \tag{2.3}$$

The most important and distinctive characteristic of polymer brushes expressed in Eq. (2.3) is that the equilibrium thickness varies linearly with the degree of polymerization. This is in contrast with free polymer chains in a good solvent, in which the dimension of polymer chain varies with N in a relationship of $R \sim N^{3/5}$ [33]. This is also very different from the behavior of the free polymer chains in a theta solvent where polymer chains possess an unperturbed configuration, $R_0 \sim N^{1/2}$. In conclusion, theoretical considerations demonstrate that the densely tethered polymer chains are deformed. The relationship between the equilibrium thickness and degree of polymerization of polymer chains is linear. This is the origin of the novel behavior of tethered polymer brushes.

The idea of the balance of interaction energy and elastic free energy, the essential features in the Alexander model, can be applied to other situations involving polymer brushes in a theta solvent or a poor solvent [34]. In a theta solvent, the interaction between statistical segments disappears. The free energy per chain is expressed in the following equation:

$$F/kT = w\varphi^3 d^2 L/a^3 + L^2/Na^2 \tag{2.4}$$

where w is a dimensionless third virial coefficient. The relationship between the equilibrium thickness and N can be obtained by minimization of free energy with respect to L.

$$L/a \approx N(a/d) \tag{2.5}$$

It is interesting to see that the linearity of L with N is maintained in theta solvents and poor solvents. Compared to Eq. (2.3), the chains have shrunk by a factor of $(a/d)^{1/3}$, but polymer chains are still distorted at the theta point. This is remarkably different from the behavior of free polymer chains in theta solvents, where the relationship between chain dimension and N is $R_0 \sim N^{1/2}$.

For a brush without solvent (melt brush), the relationship between the thickness of polymer brushes and degree of polymerization can be obtained by a similar approach. It was found that the relationship can be described in the following equation:

$$L \sim N^{2/3} \tag{2.6}$$

As indicated in Eq. (2.6), the tethered polymer chains in the melt state are deformed compared with the behavior of free polymer chains in melt state, where the relationship is $R_0 \sim N^{1/2}$.

In conclusion, no matter whether in the presence of a good solvent, a theta solvent, a poor solvent, or in the absence of solvent (melt conditions), the polymer chains in tethered polymer brushes exhibit deformed configurations. The degree of deformation of polymer chains depends on the environmental conditions to which tethered polymer chains are exposed. Deformed configurations are found under

equilibrium conditions. The relationship between the number of statistical segments N and the dimension of tethered and free polymer chains (L and R_g, respectively) under various conditions is summarized in the Table 1 for comparison.

The Alexander approach is a simple free energy balance argument. It does not attempt to examine the details of the conformations of polymer chains or the density profile of chain units at a distance from the grafting surface. This simple model can be used to describe the hydrodynamic properties of polymer brushes and other properties, which depend on perturbing the balance between chain stretching and chain–chain repulsion. Such properties are the hydrodynamic thickness, permeability of a brush and the force per area required to compress a brush (either vertically or laterally). The lubrication forces that arise when two brushes are brought into near contact are related to the hydrodynamic properties.

However the following questions on brush structures are not well represented by the Alexander model. These questions include: the shape of the chain unit density, the location of the free ends of polymer chains, how the polymer chains segregate or mix in a mixed polymer brush of either different chain lengths or different chemical compositions and how the polymer chains interpenetrate each other. Considerable theoretical work beyond the simple Alexander model has been devoted to understanding the detailed structure of polymer brushes. Relatively simple theoretical results have been obtained for a wide variety of brush properties and situations under the conditions of strong stretching. A simple hypothesis about free chain ends from the interface is made: the free chain ends may be located at any distance from the interface [1,35–38]. This is different from the Alexander model in which all chain free ends are located at the same distance from the interface. The results show that the potential of a chain is a parabola. All of the properties of the more detailed "parabolic" brush description are consistent with the scaling analysis of the Alexander model argument.

2.2. Experimental studies of flexible homopolymer brushes

Experimental research has been carried out to elucidate polymer brush structures and explore their novel properties. However it is not easy to design a very good polymer brush system and experimental method to check the theoretical predictions. For end-adsorbed polymer brushes, optical probes such as evanescent waves [39], ellipsometry [40], infrared spectroscopy [41] and multiple-reflection interferometry [42,43] have given information equivalent to the total amount of polymer adsorbed. Many scattering experiments have been performed to investigate the structure of end-grafted polymer systems. The variation of chain unit density as a function of the distance from the tethering interface and how structure properties change with the quality of the solvent were studied. Cosgrove et al. [44,45] performed neutron scattering experiments on short (average molecular weight $M_n \approx 5000$ g/mol) poly(ethylene oxide) chains end-grafted to 100 μm latex spheres in suspension. Neutron scattering has ample spatial resolution to observe features of the density profile. The results compared favorably to numerical calculations. Parsonage and coworkers [46] studied the adsorption of the diblock copolymer polystyrene-*b*-poly(4-vinylpyridine) (PS-*b*-PVP) from toluene solution onto mica and used radiolabeling techniques to measure the coverage for various PS-*b*-PVP copolymers on mica. With fixed PVP chain lengths, they found roughly constant coverage over a range of PS chain lengths and found brush heights scaling as N. This was consistent with predictions from the Alexander model (Flory argument). Patel et al. [47] studied a series of adsorbed block copolymers where a block strongly interacts with the surface and the other block adsorbs weakly. They determined the layer thickness from the range of the onset of detectable repulsive force exerted between the layers. The experimental results showed that for

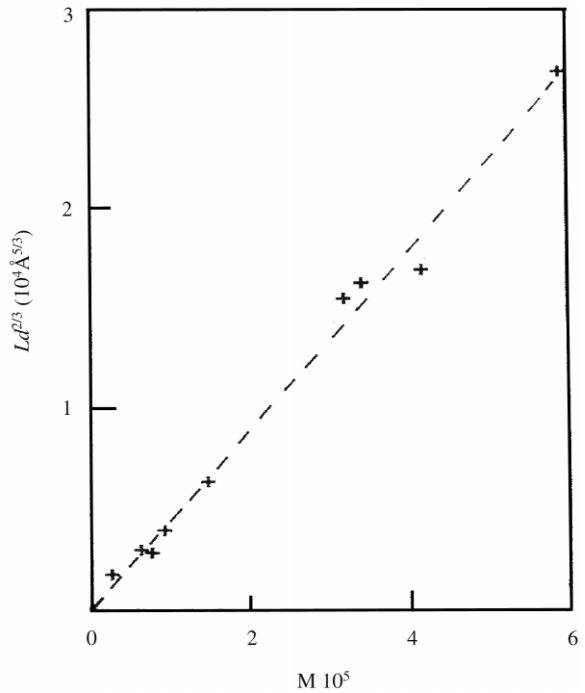

Fig. 3. Plot of $Ld^{2/3}$ vs M for grafted PDMS in a good solvent (dichloromethane) [48].

a series of copolymers of nearly constant *d* and variable *N* of the weakly adsorbed block, linearity of *L* with *N* was observed.

The work of Auroy et al. [48] gave strong support of linearity of polymer brush height with respect to the degree of polymerization of tethered polymer chains. To prepare a large amount of brush as a scattering target, they chemically end-grafted polydimethylsiloxane (PDMS) chains on porous silica particles and performed neutron scattering. Information about the total amount of adsorbed polymer and brush height was extracted from the raw data. Their results in CH_2Cl_2, a good solvent for PDMS, are illustrated in Fig. 3. It showed not only the linearity of the layer thickness vs. molecular weight over more than a 30-fold variation in *N*, but also a good agreement with the predicted inverse 2/3 power dependence on *d*. Molecular dynamics simulation work of Murat and Grest [49–51] also supported the results of the Flory argument. It is expected that more experimental data will be reported with the results of newly developed experimental methods.

2.3. Theoretical studies of semiflexible polymer brushes, liquid crystalline polymer brushes, charged polymer brushes and binary polymer brushes

Semiflexible polymer brushes [52], liquid crystalline polymer brushes [53–60], charged polymer brushes [61–66] and binary polymer brushes [26] have also been studied from a theoretical point of view. For semiflexible polymer brushes on a flat substrate, polymer backbone structures are more persistent and the segment–segment interactions would have directional components. These persistent polymer backbones can be found in many synthetic polymers and biological macromolecules like DNA

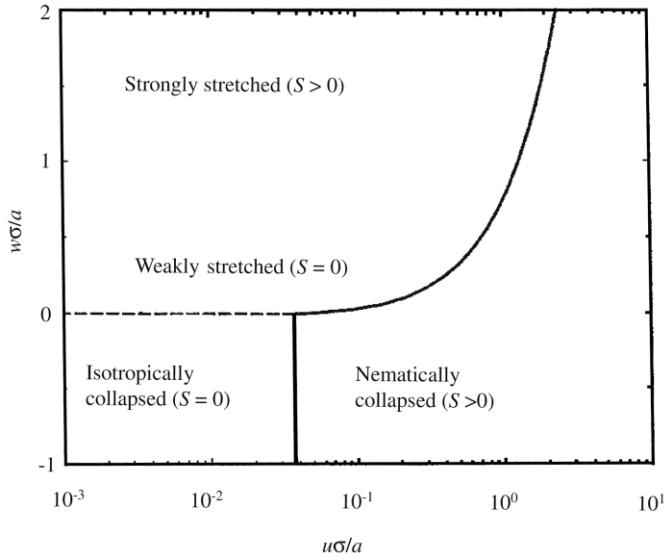

Fig. 4. Phase diagram for semiflexible polymer brushes in terms of the reduced isotropic interation $w\sigma/a$ versus the reduced anisotropic interaction parameter $u\sigma/a$ [52].

and RNA. The situation is different from that of flexible polymer brushes, where segmental interactions are considered to be directionally isotropic. The coupling between the angular and concentration distributions of the segments of a semiflexible polymer brush would yield many interesting features unique to persistent chains. An interesting question in a long semiflexible polymer brush is the possibility of forming a liquid-crystalline polymer brush. For spatially homogeneous worm-like chains in a good solvent, it is known that orientational interactions are responsible for inducing an isotropic–nematic phase transition [59].

The phase diagram for semiflexible polymer brushes in terms of the reduced isotropic interaction parameter $w\sigma/a$ vs. the reduced anisotropic interaction parameter $u\sigma/a$ is presented in Fig. 4 [52]. Here σ is the surface grafting density, a is the bond length, u represents the coefficient of an anisotropic interaction and w is a segmental excluded volume. The solid curve describes first-order transitions between different regimes, while the dashed curve represents a smooth crossover between the isotropically collapsed and stretched states. The phase diagram shown in Fig. 4 consists of four regimes: (i) strongly stretched brushes with the orientation order parameter $S > 0$ and the brush height $L > Na/3$, where N is the number of segments; (ii) weakly stretched brushes with $S = 0$ and $L \sim (w\sigma/a)^{1/3} \ll Na/3$, where w is the segmental excluded volume; (iii) isotropically collapsed brushes with $S \approx 0$ and $L \sim (\sigma v/|w|)N \ll Na$, where w and v are the second and third virial coefficients of the segmental interactions; and (iv) nematically collapsed brushes with $S > 0$ and $L \sim (\sigma v/|w|)N \ll Na$. The first-order isotropic–nematic phase transitions between isotropically and nematically collapsed brushes, and between stretched and nematically brushes have been predicted by a scaling theory.

The phase transition behavior of liquid crystalline polymer brushes has been investigated [53–58]. Pickett and Witten [57] studied the thermal transition in liquid crystalline polymer brushes in the absence of solvent. Using the simple Alexander model, Mercurieva et al. [58] investigated a swollen brush with thermotropic mesogenic groups in polymer chains. The liquid crystalline polymer brushes

exhibit a discontinuous phase transition, which is similar (or even identical) to the transition in a polymer solution, or alternatively a continuous transition depending on the grafting density of the brush. Amoskov et al. [53,55] reported a theoretical study of liquid crystalline ordering in planar polymer brushes formed by macromolecules with mesogenic groups in the main chains and immersed in a solvent. Using numerical calculations with a SCF approximation, they found the existence of a microphase-segregated brush regime with a collapsed orientationally ordered intrinsic sublayer and a swollen external sublayer. The transition from a conventional brush state to the microphase-segregated state is continuous at high grafting density. At small grafting density this transition is a jump-wise first order transition for finite chain length (N). The magnitudes of the jumps in the average characteristics of the brush tend toward zero in the limit $N \rightarrow \infty$. Amoskov et al. [54] also studied the interaction of liquid crystalline polymer brushes oriented face to face under compression and subsequent extension. It was shown that contact between liquid crystalline brushes composed of folds of grafted chains led to interpenetration of brushes and formation of a combined structure. The brushes appeared to be glued together and remained joined even if the grafting surfaces were forced apart.

The behavior of charged polymer brushes (polyelectrolyte brushes) is another intriguing research area [61–66]. This polymer brush system is more complex because of the introduction of electrostatic interactions between the grafted polymer chains. Scaling analysis of planar polyelectrolyte brushes revealed a much more complex behavior than that of neutral brushes [61,66]. Pincus's study [66] showed that a polyelectrolyte brush exhibits two different types of behavior depending on the degree of charge on the chain and grafting density. It can be strongly charged, loosing its mobile counterions, which leads to the scaling relationship of brush height and N as $L \sim N^3$ (Pincus regime). Or it conserves the counterions mainly inside the brush, thus, being practically electroneutral (osmotic regime). If a salt is added into the solution and the salt concentration in solution is much higher than the concentration of counterions in the brush, then a third regime (salt brush) is formed. The behavior of a polyelectrolyte in this regime is very similar to that of a neutral brush, although the electrostatic interaction is dominant. The interactions in the brush can be described by an effective second virial coefficient incorporating both nonelectrostatic and electrostatic interactions. Israels et al. [65] described numerical results from an SCF model for the structure and scaling behavior of charged polymer brushes. Their studies showed that "Pincus regime" is too small to be detected.

Binary polymer brushes have also been extensively studied [26,60,67–70]. Marko et al. [60,66] used the SCF theory to examine the equilibrium properties of a binary polymer brush composed of immiscible chains under melt conditions. For two homopolymers with sufficiently high immiscibility, two possible ordered phases were studied: a "rippled" phase described in terms of a "density wave" in composition directed along the surface, which was equivalent to lateral microphase separation; and a "layered" phase rich in one component at the bottom of the brush and rich in the second component at the top of the brush. Their results showed that the lateral transition was expected to be the one observed. Soga et al. [26] used a coarse-grained simulation method that involved direct calculation of the Edwards Hamiltonian to study the behavior of binary polymer brushes in a solvent. They found that if two components were sufficiently immiscible, lateral binary microphase separation occurred over a wide range of solvent conditions. The onset of phase separation was delayed as solvent quality increased. Under poor solvent conditions they found interesting structural variations as a result of the combination of phase separation from solvent and phase separation of the two components.

Although extensive theoretical research work has been carried out on semiflexible polymer brushes, liquid crystalline polymer brushes and binary polymer brushes, few experimental results regarding these polymer brushes have been reported.

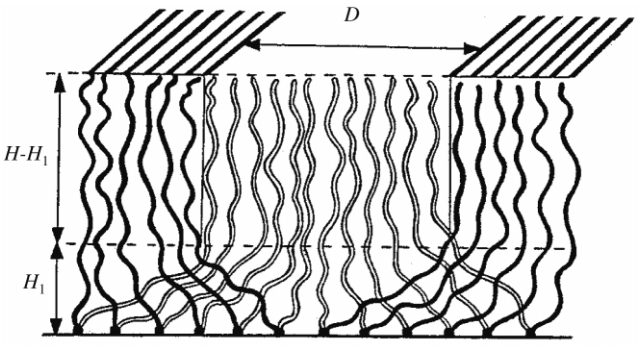

Fig. 5. Laterally microsegregated brush formed by Y-shaped block copolymers. Reprinted with permission from Macromolecules 1996;29:2667. © 2000 American Chemical Society [73].

3. Theoretical studies of tethered copolymer brushes

Extensive theoretical work on the behavior of the copolymer brushes has been reported in the past several years [25,71–77]. By changing chain architecture, grafting density, whole chain length, relative chain length, interaction energy between different blocks and interaction energies between blocks and solvents, a variety of novel well-ordered structures such as “onion”, “garlic”, “dumbbell”, flowerlike and checkerboard have been predicted using the mean field method, scaling arguments, Monte Carlo simulations and SCF lattice calculations [25,72–75]. The theoretical results indicate that tethered copolymer brushes on a flat substrate are an excellent candidate for forming patterned polymer films.

Using a mean field method, Dong et al. [71] studied the phase behavior of densely tethered diblock copolymers in the melt state and observed distinct patterns of phase separation. Unique structures have also been noted in polymer brushes where attractive functional groups are attached to the free ends of the chains [78,79]. A “layering effect” was observed; the functional groups were localized in a layer at the top of the brush. Gersappe et al. [76] used Monte Carlo simulations and numerical SCF lattice calculations to study the behavior of copolymer brushes. By varying the sequence distribution of tethered linear AB copolymers, they found that brushes composed of block copolymers showed distinct lateral inhomogeneities, with large domains of A and B units. The size of these domains appears diminished in random copolymer brushes. The alternating copolymer brushes do not exhibit distinctive domains like those in block copolymer brushes. Tethered diblock copolymer brushes are predicted to form patterns under specific conditions, theoretical considerations will be reviewed in Sections 3.1 and 3.2.

3.1. Pattern formation from tethered Y-shaped copolymer brushes

Zhulina and Balazs [73] used theoretical models to study the pattern formation for a tethered Y-shaped AB copolymer on a flat surface. The model is described as follows: (i) the stem of the Y is just one site in size and serves to tether macromolecules to the surface; (ii) one arm of the Y is an A homopolymer chain, while the other arm is an incompatible B homopolymer; and (iii) both A and B

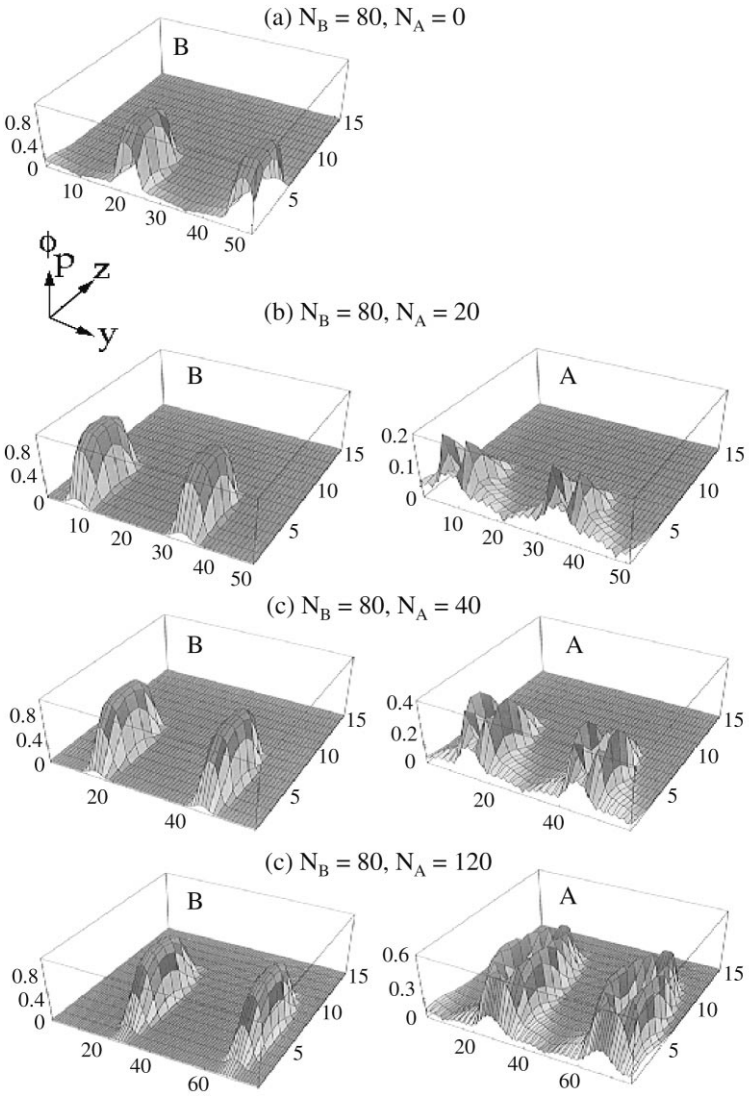

Fig. 6. The plots reveal the effect of increasing N_A, while keeping N_B fixed at 80. The diblock copolymers are grafted by the more soluble A component. The other parameters are set at $\chi_{BS} = 2$, $\chi_{AS} = 1$ and $\chi_{AB} = 0$. Y refers to the grafting direction and ϕ_P denotes the polymer density. The plots marked B show the polymer density of the B blocks, while the plots marked A show the density of the A blocks. Reprinted with permission from Macromolecules 1996;29:6338. © 2000 American Chemical Society [72].

are assumed to be flexible and identical in length. The size of each monomer is given by a. The tethering density of the copolymer chains is $(1/s)$, where s is the area per polymer chain. The polymer brush is immersed in a solvent and the solvent is assumed to be nonselective, i.e. it is of the same quality for both components A and B. The behavior of the chains at both high and low grafting densities was considered.

Due to the interplay between A, B and solvents, the microphase segregation in this system is governed

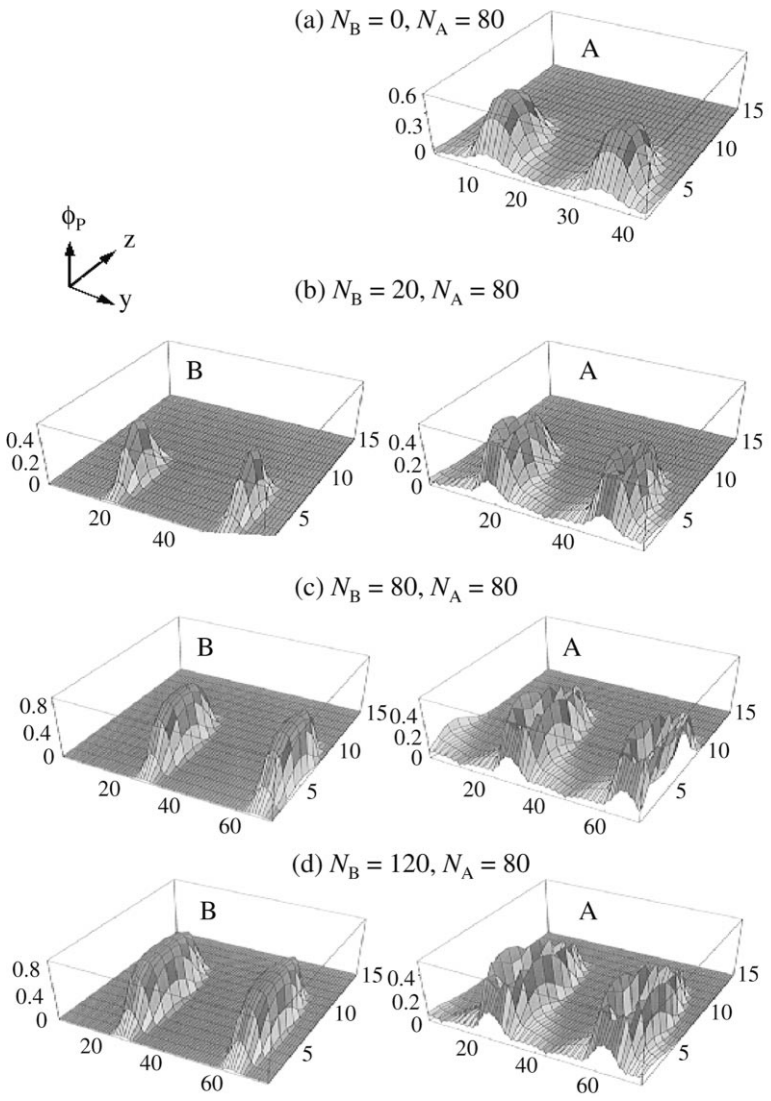

Fig. 7. The plots reveal the effect of increasing N_B, while keeping N_A fixed at 80. The copolymers are grafted by the more soluble A component. The other parameters are set at $\chi_{BS} = 2$, $\chi_{AS} = 1$ and $\chi_{AB} = 0$. Y refers to the grafting direction, and ϕ_P denotes the polymer density. The plots marked B show the polymer density of the B blocks, while the plots marked A show the density of the A blocks. Reprinted with permission from Macromolecules 1996;29:6338. © 2000 American Chemical Society [72].

not only by N and χ but also tethering density. The study focused on the case of poor solvents. In this situation the polymer chains undergo lateral segregation. Coupling this phase behavior with the incompatibility between A and B, which is characterized by χ, can further drive the chains to form a variety of unique morphologies. In the case where the grafting density is relatively high, the thickness of the brush is given by $L = Na^3/s$. They also assumed that the brush was subdivided into two horizontal sublayers of

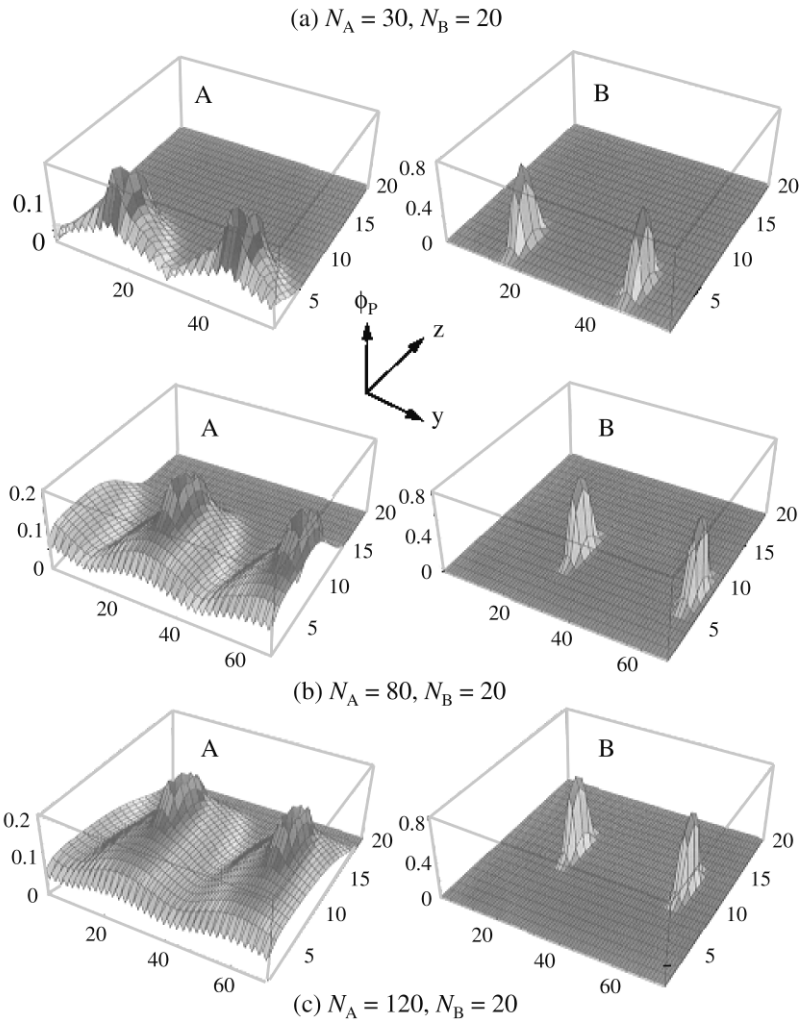

Fig. 8. 3D plots showing the effect of increasing N_A while keeping N_B fixed at 20 for diblock copolymers grafted by the soluble A block: (a) $N_A = 30$; and (b) $N_A = 120$. $\chi_{BS} = 2$, $\chi_{AS} = 0$, $\chi_{AB} = 0$. Y refers to the grafting direction and ϕ_P is the polymer density. The plots marked B show the density of B block, while the plots marked while the plots marked A show the density of A blocks. Reprinted with permission from Macromolecules 1996;29:8254. © 2000 American Chemical Society [74].

thickness H_1 and $(H - H_1)$ (see Fig. 5). The lower sublayer contains randomly mixed segments of the A and B chains. The upper layer consists of microsegregated domains of A and B, which form regular, alternating "stripes". $N - n$ and n are used to denote the average number of units per block localized in the upper and lower sublayers. The width is D, and thus the periodicity is $2D$. In the cases of poor solvents, solvent quality is taken into account and a new parameter τ is introduced. This parameter τ is a measure of the relative deviation from the Θ temperature, $\tau = (\Theta - T)/\Theta$. The results are shown in the following equations:

$$n = (N/\chi\tau)^{1/2} \tag{3.1}$$

$$H_1 = N^{1/2} s^{-1} \chi^{-1/2} \tau^{-3/2} \tag{3.2}$$

$$D = aN^{1/2} \tag{3.3}$$

These equations indicate that increasing χ results in an increase in the thickness of the segregated sublayer. However, χ does not affect the value of d. At low grafting density, a "sparse" brush forms. The brush loses its lateral homogeneity and splits into separate coils in good or theta solvents or aggregates into "pinned micelles" or "octopus" structures in poor solvents. The pinned micelles could be mixed micelles, internally segregated micelles, or split micelles depending on the interaction parameter between chains A and B. Higher χ results in split micelles and the layer self-assembles into a checkerboard pattern.

3.2. Pattern formation from tethered diblock copolymer brushes

Zhulina et al. [72] continued their studies on forming patterned films by considering the behavior of tethered linear flexible AB diblock copolymer brushes in a poor solvent. In this study, they mainly considered the situation where χ_{AB} is close to zero, but the solvent affinities of different blocks are significantly different. Under these assumptions, the behavior of polymer brushes is determined by polymer–solvent interactions. Both SCF calculation and scaling arguments were employed to study the pattern formation from these polymer brushes.

The grafting density is given by $1/s$, where s is the area per chain. The diblock copolymer chains contain $N_A \gg 1$ and $N_B \gg 1$ units of size a. The brush is immersed in a poor solvent for both components. The values of the second virial coefficients are negative, which means the contact between like monomers are attractive. It is assumed that the interactions between both blocks and surface are the same as that with the solvent. Thus, the system behavior can be described by two parameters, $\tau_A = (1 - \chi_{AS})/2$ and $\tau_B = (1 - \chi_{BS})/2$, where χ_{AS} and χ_{BS} are the Flory–Huggins parameters for the respective polymer–solvent interactions. The study focused on relatively sparse grafting density. To obtain a clear picture, the following parameters were assumed: the grafting density per line along x is 0.025, $\chi_{AB} = 0$, $\chi_{AS} = 1$ and $\chi_{BS} = 2$. The results from SCF calculations are shown in Figs. 7 and 8.

For brushes in which polymer chains are tethered by the less soluble block, the copolymer chains associate into "onion" structures, where the less soluble B's form the inner core and the more soluble A's form the outer layer to shield the B's from the unfavorable solvent. Even for small N_A, this structure is favored. As N_A is increased, the polymer density within the shell increases and the B cores are more effectively shielded from the solvent. Further increasing N_A does not change the density but enhances the lateral and vertical extent of the A coating.

For brushes in which chains are tethered by the more soluble block, each A block contributes to form the leg of the micelles whose core consists of the less soluble B blocks (see Fig. 6). As N_A is increased the legs become less stretched, and A blocks form a shield around the core to minimize the unfavorable contacts between the solvent and B blocks. Further increases in N_A make the shielding of A blocks around B blocks more effective. At the same time, the B block cores are pushed away from the tethering surface. Here the number of chains in a micelle f is more sensitive to N_A than the previous case. The changes when N_A is fixed, while N_B is increased are also considered. The calculation results from two-dimensional SCF are shown in Fig. 7. At small N_B, the core is small and effectively shielded by A blocks in all directions. As N_B increases, the size of the micelles is increased; further increasing N_B decreases the density of A around B

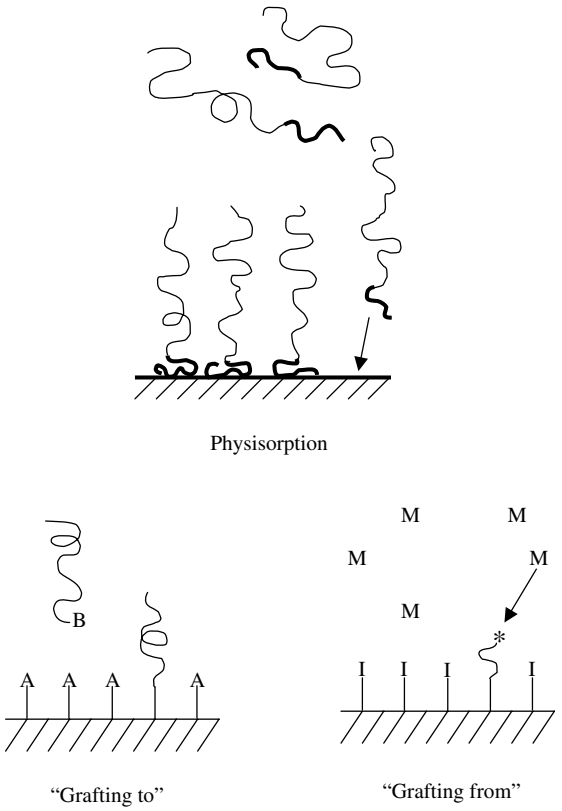

Fig. 9. Preparation of polymer brushes by "physisorption", "grafting to" and "grafting from".

core. The density of the core initially increases with the length of B; however, once N_B is sufficiently long, the core density depends only on the value of χ_{BS} and becomes independent of N_B.

Through scaling theory, they determined how the size and shape of the micelle structures vary with the solvent quality and the properties of the diblocks. A diagram was determined to delineate where these different structures appear as a function of the relevant parameters. In the case where the solvent is a theta solvent or good solvent for one block but is a poor solvent for another block, it is expected that the self-assembly will be affected by the swelling of the solvophilic component, and the morphology will be different from the previous case [74]. In this case, the surrounding solvent is a theta solvent or a marginally good solvent for A blocks (i.e. $\tau_A = (T - \Theta_A)/T \geq 0$) and a poor solvent for B blocks (i.e. $\tau_B = (\Theta_B - T)/T > 0$). Θ_A and Θ_B are the corresponding theta temperatures for A and B blocks. The Flory–Huggins interaction parameter between A and B blocks, χ_{AB}, is assumed to be zero.

It is easier to visualize the micelle formation by three-dimensional (3D) plots obtained from SCF calculations. The density profiles provide a picture of local concentration gradients in the system. Fig. 8 displays the graphic output from the SCF calculations. The figure shows the effect of increasing N_A while keeping N_B fixed at 20 for diblock copolymer grafted by the soluble A block. When the length of the soluble A block is small, the layer is laterally homogeneous; the A chains are too short to stretch and aggregate with each other. As N_A is increased, B blocks form a core; A blocks stretch and form a shell around the B core to reduce the unfavorable contacts between B and solvents. Further increasing N_A

makes A blocks form a polymer brush. As expected for planar brushes, the micelles formed by B blocks move away from the grafting surface (Fig. 8b and c).

For the chains tethered by less soluble B blocks, B blocks form a dense micellar core and the soluble A blocks form a shield around the B cores. The structure resembles a "flower" whose core is formed by B blocks and the "petals" are formed by the A blocks.

If the grafting is relatively uniform, the micelles self-assembled from the tethered diblock copolymer brushes will form an ordered array or pattern on the surface. Also the size and spacing of micelles, and thus the dimension of the pattern can be controlled by tuning various parameters such as N_A, N_B, χ_{AB}, χ_{AS}, χ_{BS} and grafting density. These patterned polymer films could be useful in many applications, including tailoring surface properties for wetting, friction protection, information technology, and micro- or nano- reactors.

4. Synthesis of polymer brushes

This section describes the preparation of polymer brushes on solid substrate surfaces (impenetrable interfaces). Generally, there are two ways to fabricate polymer brushes: physisorption and covalent attachment (see Fig. 9). For polymer physisorption, block copolymers adsorb onto a suitable substrate with one block interacting strongly with the surface and the other block interacting weakly with the substrate. Covalent attachment can be accomplished by either "grafting to" or "grafting from" approaches. In a "grafting to" approach, preformed end-functionalized polymer molecules react with an appropriate substrate to form polymer brushes. The "grafting from" approach is a more promising method in the synthesis of polymer brushes with a high grafting density. "Grafting from" can be accomplished by treating a substrate with plasma or glow-discharge to generate immobilized initiators followed by polymerization. However "grafting from" well-defined self-assembled monolayers (SAMs) is more attractive due to a high density of initiators on the surface and a well-defined initiation mechanism. Also progress in polymer synthesis techniques makes it possible to produce polymer chains with controllable lengths. Polymerization methods that have been used to synthesize polymer brushes include cationic, anionic, TEMPO-mediated radical, atom transfer radical polymerization (ATRP) and ring-opening polymerization. In the following section, the emphasis will be put on the synthesis of polymer brushes from SAMs.

4.1. Preparation of polymer brushes by physisorption

Tethering of polymer chains onto a solid surface could be a reversible process or irreversible process. Irreversible grafting is accomplished by chemical bonding, this method includes "grafting to" and "grafting from". Physisorption is a reversible process and is achieved by the self-assembly of polymeric surfactants or end-functionalized polymers on a solid surface [80]. The surface grafting density and all other characteristic dimensions of the structure are controlled by thermodynamic equilibrium, albeit with possible kinetics [2].

Physisorption of block copolymer or graft copolymer occurs in the presence of selective solvents or selective surfaces, giving rise to selective solvation and selective adsorption, respectively. The detailed polymer brush structure depends on the selectivities of these media and the nature of the copolymers, the architecture of copolymers, the length of each block and the interactions between blocks and surface. In

the case of selective solvents [46], an ideal solvent is a precipitant for one block which forms an "anchor" layer on the surface and a good solvent for other block which forms polymer brushes in the solution. In the case of a selective surface [81,82], one block is preferentially adsorbed on the surface and another one forms a polymer brush. Many papers have been published in the field of physisorption of block copolymers; various techniques have been employed to probe the brush structures. We have selected some representative examples to illustrate this method.

Parsonage et al. [46] studied a series of polymer brushes prepared by adsorption of 18 PS-*b*-PVP block copolymers of various molecular weights. Toluene is a selective solvent for PS-*b*-PVP; PVP blocks formed an anchor layer on the surface while PS blocks formed a brush. Their results showed that for all but the copolymer of highest asymmetry, the measured adsorption density was in good agreement with the theoretical studies. For highly asymmetric copolymers, the large relative size of the nonadsorbing blocks played a significant role in reducing the surface adsorption density.

In the study of Fytas et al. [83], PS-*b*-PEO block copolymer was adsorbed on a glass prism surface to form a PEO anchor and PS buoy. Toluene is a good solvent for both blocks; polar PEO blocks showed a stronger attraction to the surface than the nonpolar PS blocks. The brush was formed by the stretched PS blocks. A copolymer concentration greater than the threshold value for maximum adsorbance was used. They used evanescent-wave dynamic light scattering to probe the thermal fluctuations of the segment density profile of the brush (dynamic structure of polymer brushes). Experimental results revealed the presence of long-lived, thermally induced layer fluctuations and strong surface effects on thermal decay rate.

Field et al. [84] used specular neutron reflection to investigate the density profile of PS-*b*-PEO block copolymer adsorbed from toluene-d_8 onto a quartz surface. The results showed that the reflectivity profiles were well described by a parabolic or error function for polymer density profiles normal to the interface. Using the same copolymer, PS-*b*-PEO, to form polymer brushes on silicon wafers by adsorption from toluene, Motschmann et al. [85] studied the adsorption kinetics and adsorption isotherm. Their experimental results revealed that the adsorption kinetics show two processes on a clearly separated time scale. In the beginning, the adsorption process was diffusion controlled, leading to a surface coverage with small interaction between chains. A denser brush was formed by the penetration of chains through the existing monolayer combined with the conformation rearrangement.

Atomic force microscopy (AFM) was used to study the polymer brushes reported by Kelly et al. [86]. Adsorption of PS-*b*-PVP on mica was achieved in toluene, while adsorption of poly(4-*tert*-butylstyrene-*b*-poly(sodium styrene-4-sulfonate) (PtBS-*b*-NaPSS) on mica was accomplished in aqueous solution. Force–distance (F–D) profiles of PS-*b*-PVP in a good solvent and a series of F–D profiles of PtBS-*b*-NaPSS as a function of aqueous NaCl concentration were obtained. AFM F–D profiles of the second brush showed a strong dependence of interaction distance on NaCl. Images showed that the chain density is not uniform.

Preparation of polymer brushes by adsorption of block copolymer from a selective solvent (or on selective surface) is not difficult. However, the polymer brushes exhibit thermal and solvolytic instability due to the weak interactions between the substrate and the block copolymers [87]. The interactions in most cases are van der Waals forces or hydrogen bonding. Desorption could occur upon exposure to other good solvents or the adsorbed polymers are displaced by other polymers or other low molecular weight compounds. If these polymer ultrathin films are heated to a high temperature (e.g. above glass transition temperature or melting temperature), dewetting occurs and polymer films are no longer homogeneous due to formation of polymer droplets [88,89]. Also, it is not always easy to synthesize block copolymers, which are suitable for physisorption. Some of these drawbacks could be overcome by covalently tethering polymer chains to substrates.

4.2. "Grafting to" approach to fabricate polymer brushes

"Grafting to" approach refers to preformed, end-functionalized polymers reacting with a suitable substrate surface under appropriate conditions to form a tethered polymer brush. The covalent bond formed between surface and polymer chain makes the polymer brushes robust and resistant to common chemical environmental conditions. This method has been used often in the preparation of polymer brushes. End-functionalized polymers with a narrow molecular weight distribution can be synthesized by living anionic, cationic, radical, group transfer and ring opening metathesis polymerizations. The substrate surface also can be modified to introduce suitable functional groups by coupling agents or SAMs.

Koutsos et al. [90,91] synthesized a series of thiol-terminated polystyrenes with a low polydispersity (<1.2) by anionic polymerization and prepared chemically end-grafted polystyrene chains on a gold surface by exposing the gold substrate to a toluene solution of these polymers. AFM was used to study the polymer conformation of these end-grafted polystyrenes in bad solvents (water). Microphase separation of polymer monolayer into globular clusters was observed at higher surface coverage and it was found that the sizes of these clusters were consistent with the scaling laws, which were predicted for pinned micelles.

Mansky et al. [27] synthesized a series of hydroxy-terminated random copolymers of styrene and methyl methacrylate with different ratios by a "living" radical polymerization. These end-functionalized polymers were reacted with silanol groups on the silicon wafer surface under vacuum at 140°C to form tethered random copolymer brushes. They found that a random copolymer brush with a specific composition provided a surface with no preferential affinity for either PS component or PMMA component. This surface has been successfully used to control the domain orientation of PS-*b*-PMMA films spin coated on this copolymer brush surface.

Using a similar strategy, Bergbreiter et al. [92] tethered terminally functionalized poly(*tert*-butyl acrylate) onto oxidized polyethylene films. Yang et al. [93] prepared vinyl-terminated SAMs on silicon surfaces and used hydrosilation reaction to covalently tether poly(methylhydrosiloxane) and its derivatives onto the solid surface. Ebata et al. [94] synthesized end-grafted polysilane on quartz surfaces by the "grafting to" approach and characterized the tethered polysilane by UV spectroscopy. Poly(amidoamine) dendrimers were also successfully tethered to a mercaptoundecanoic acid SAM [95]. Tran et al. [96] studied the structure of polyelectrolyte brushes that were prepared by the attachment of trichlorosilyl-functionalized PS to a substrate followed by sulfonation of the tethered PS.

Frank et al. [97] prepared surface-immobilized polymer films by a photochemical process. A silicate surface was modified with 4-(3′-chlorodimethylsilyl)propyloxybenzophenone followed by deposition of a polystryrene or poly(ethyloxazoline) film. Illumination with UV light produced a covalently bound film via a photochemical attachment. Typically, several nanometers of polymeric overcoat could be attached.

In general, only a small amount of polymer can be immobilized onto the surface by "grafting to" approach. Macromolecular chains must diffuse through the existing polymer film to reach the reactive sites on the surface. This barrier becomes more pronounced as the tethered polymer film thickness increases. Thus the polymer brush obtained has a low grafting density and low film thickness. To circumvent this problem, investigators have used the "grafting from" approach, which has become more attractive in preparing thick, covalently tethered polymer brushes with a high grafting density.

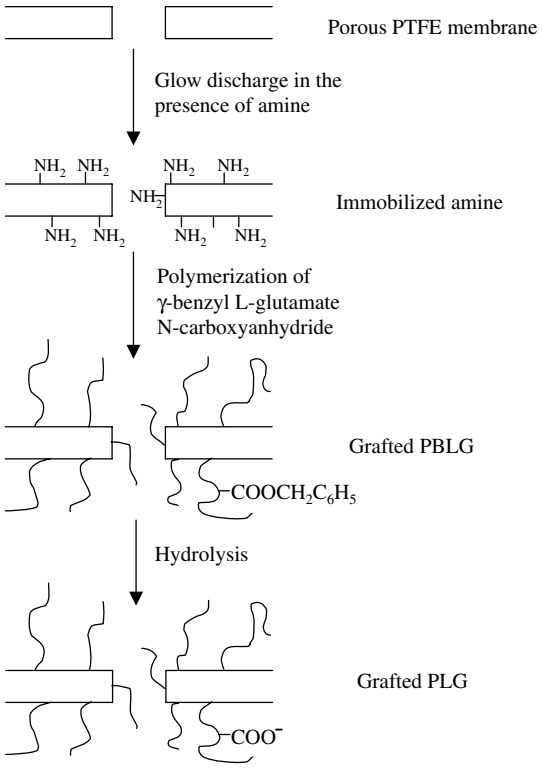

Fig. 10. Synthesis of polyglutamic acid (PLG) brushes on a porous PTFE membrane. The amine initiator is introduced onto membrane by glow discharge. Reprinted with permission from J Am Chem Soc 1997;119:1619. © 2000 American Chemical Society [16].

4.3. "Grafting from" approach to synthesize polymer brushes

The "grafting from" approach has attracted considerable attention in recent years in the preparation of tethered polymers on a solid substrate surface. The initiators are immobilized onto the surface followed by in situ surface initiated polymerization to generate tethered polymers. The immobilization of initiators on the substrate surface can be achieved by treating the substrate with plasma or glow-discharge in the presence of a gas or forming initiator-containing SAMs on the substrates.

4.3.1. Synthesis of tethered polymers from plasma- or glow-discharge-treated substrates

It is easy and convenient to use plasma and glow-discharge treatment to introduce initiators onto substrate surfaces [16–18,98–102]. Ito et al. [16] subjected a porous PTFE membrane to a glow-discharge using a high frequency modulator (400 W) in the presence of ammonium gas at a pressure of 0.5 Torr (see Fig. 10). The amino groups were immobilized on the surface, the number of amino groups was determined by ninhydrin. It was found that the density of amino groups on the surface increased with increasing power and time of the glow-discharge treatment. The immobilized amino groups initiated the polymerization of γ-benzyl L-glutamate *N*-carboxyanhydride to produce tethered polymers on the PTFE membrane. Hydrolysis of the tethered poly(γ-benzyl L-glutamide) afforded

poly(glutamic acid) brushes. The modified membrane was used as a pH-sensitive chemical gate. Using the same strategy, they grafted poly(methacrylic acid) (PMAA) on a porous polycarbonate membrane [17,98] and grafted poly[3-carbamoyl-1-(*p*-vinylbenzyl)pyridinum chloride] (PCBVP) on a porous PTFE membrane [18]. The PMAA brush modified membrane was also used as a pH-sensitive gate. The PCVBP brushes modified membrane was used in oxidoreduction-sensitive control of water permeation.

Park et al. [99] glow-discharged a porous glass filter treated with octadecyldimethyl-*N*,*N*-diethylaminosilane in the presence of air. Peroxide groups were introduced onto the surface. Heating the treated substrate in a dimethylformamide (DMF) solution of a spiropyran-substituted methyl methacrylate and methyl methacrylate at 60°C for 4 h produced a tethered copolymer. This copolymer brush modified porous glass filter was used for photocontrolled gating because the pendent spiropyran isomerized to the merocyanine group upon ultraviolet light irradiation. This change led to a different solubility of the tethered copolymer in toluene. The zwitterionic merocyanine form of tethered copolymer contracted in toluene. Therefore the permeability was controlled through UV irradiation. In a publication by Yamaguchi et al. [100], a porous polyethylene (HDPE) film was treated with an argon plasma for 60 s and was then left in contact with air for 60 min, and then in contact with the solution of *N*-isopropylacrylamide and benzo[18]crown-6-acrylamide at 80°C. Tethered copolymer was produced on the substrate surface. This polymer brush modified film could be used for a fast response molecular recognition ion gating membrane by taking advantage of the thermal sensitivity of tethered polymer and the different stability of the complex of crown ether and some ions.

However, this approach to prepare tethered polymer brushes has some drawbacks. First of all, it is not easy to control the initiator type and amount. The surface polymerization mechanism is not well defined. Compared with plasma or glow-discharge, the SAM technique to immobilize initiators on the substrate surfaces leads to a more well-defined polymerization mechanism.

4.3.2. Synthesis of tethered polymer brushes by conventional radical polymerizations

In many reported systems which used the "grafting from" method via a radical polymerization mechanism, the immobilization of radical initiators usually involved a series of steps [103–105]. An anchor molecule was immobilized on the solid substrate surface and then the initiating species was linked to the anchor molecules in one or more additional steps. For example, Boven et al. [103] treated glass beads with 3-aminopropyltriethoxysilane (γ-APS) to obtain amino functional groups on the surface. The azo initiators were then immobilized onto the surface through the formation of amide bonds between the γ-APS modified surface and an acid chloride functionalized azo initiator. Subsequent surface initiated radical polymerization produced tethered PMMA chains.

Sugawara and Matsuda [106] used a similar strategy to graft PS on poly(vinyl alcohol) film and poly(-acrylamide) on poly(ethylene terephthalate) (PET) film. First they coated the substrate with poly(allylamine) which had been partially derivatized with photoreactive phenylazido. The aminated polymer was chemically fixed on the surface the reactive phenylnitrene generated from UV irradiation. Carboxylated azo initiators were then immobilized onto the surface through a condensation reaction with immobilized aminated polymer. Radical polymerization under suitable conditions yielded tethered polymers.

Ballauff and coworkers [107] prepared spherical polyelectrolyte brushes by photoemulsion polymerization. First, a PS latex was prepared by conventional emulsion polymerization. In the second step, a seeded emulsion polymerization was performed using 2-[*p*-(2-hydroxy-2-methylpropiophenone)]-ethylene glycol-methacrylate which acts as a photoinitiator. The third step was a photoemulsion polymerization in the presence of acrylic acid. This "grafting from" process produced PS cores with a shell of

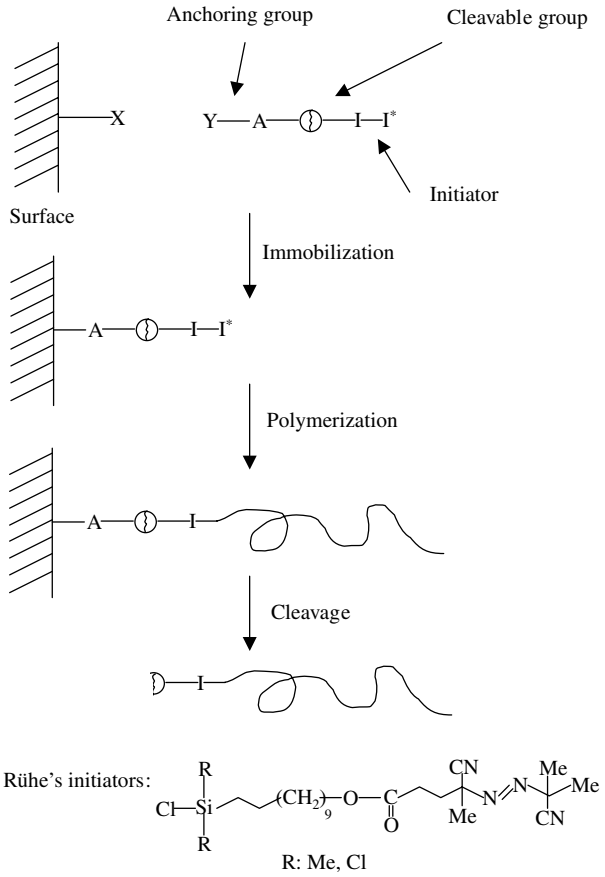

Fig. 11. Schematic description of the concept for the preparation of cleavable polymer brushes by "grafting from" approach and the initiators synthesized by Rühe et al. Reprinted with permission from Macromolecules 1998;31:592. © 2000 American Chemical Society [117].

linear poly(acrylic acid) brushes. These particles were used to test theoretical predictions of the dependence of the hydrodynamic radius on ionic strength.

Minko et al. [108–114] studied radical polymerization initiated from a solid substrate from both theoretical and experimental approaches. On the experimental side, they attached radical initiators on solid substrates such as silicon wafers, glass and ultrafine powders by either physisorption of azo or peroxide macroinitiators or chemical immobilization of azo initiators. Introduction of the covalently bound azo initiator onto a silicon wafer was performed with the method described by Tsubokawa et al. [115]. The silicon wafer was first treated with 3-glycidoxypropyltrimethoxysilane followed by the reaction with 4,4′-azobis(4-cyanvaleric acid). The surface-initiated radical polymerization was studied by in situ ellipsometric measurements of the amount of grafted chains [109]. Using the same approach, Sidorenko et al. [116] synthesized mixed or heterogeneous polymer brushes composed of PS and PVP by a two-step grafting procedure on the surface of silicon wafers. Velten et al. [19,20] attached peroxide radical initiators bearing a single cationic group to mica surfaces via ion exchange. The bound PS chains were obtained from radical polymerization of styrene under appropriate conditions.

Although these studies successfully prepared polymer brushes, there are several disadvantages. Immobilization of initiator on the surface involved several steps, which may lead to low graft densities of initiators and tethered polymers if the reactions are not quantitative. Secondly, side reactions which possibly exist in the initiator immobilization reaction may introduce some undesired structures on the surface. Accurate characterization of the initiator layer is nontrivial. This lack of knowledge about the exact composition of the initiator layer makes the understanding of polymerization mechanism difficult in some cases. It has been shown that the γ-APS layer is a very complex structure, sometimes multilayer structures may result.

To circumvent this problem, Rühe and coworkers [117–123] reported a strategy in which the complete initiator was attached to the substrate's surface in one step by SAM techniques. Fig. 11 shows this strategy. The system consisted of three components: an anchoring group A linking the initiator to the surface, the initiator (I-I) and a cleavable group (C) that allowed for degrafting of the macromolecules from the substrate for analysis. The initiator was self-assembled on the surface followed by in situ radical polymerization of styrene or other monomers by radicals generated from the bound initiator upon heating. A unique feature of this strategy was that the initiator monolayer contained a cleavable group. Therefore the tethered polymer could be degrafted and analyzed. A series of azo initiators were synthesized and immobilized on the silica gel surface. Polymerization experiments indicated this strategy had achieved great success. The kinetics of polymerization initiated from the surface bound initiator was studied by dilatometry. After polymerization the polymer was cleaved off and the molecular weight was determined. From the molecular weight, the mass of the grafted polymer and the specific surface area, the number of polymer chains per unit area was calculated and compared to the corresponding values of the initiator monolayers. It has been found that the average distance between tethered PS chains was 2–3 nm, smaller than the radii of gyration of the corresponding polymer molecules.

Using the same strategy, they also synthesized PS brushes and PMMA brushes on planar silicate substrates. These polymer brushes have been characterized by various surface characterization techniques including IR spectroscopy, surface plasmon resonance measurement, ellipsometry, X-ray reflectometry, AFM and neutron reflectometry [122]. Charged polymer brushes have attracted substantial attention in recent years in both theory and experiments.

As discussed in the theoretical consideration of homopolymer brushes, charged polymer brushes exhibit more complex behavior compared to neutral polymer brushes. Biesalski et al. [120] prepared and characterized a polyelectrolyte monolayer covalently attached to a planar solid substrate. PVP brushes were synthesized by surface initiated radical polymerization followed by quarternization of the tethered poly(4-vinylpyridine) with *n*-butyl bromide in nitromethane at 65°C. A tethered cationic polyelectrolyte monolayer [poly(4-vinyl-*N*-*n*-butylpyridinium) bromide] on flat silicate substrate was successfully prepared. The thickness of the resulting cationic monolayer can be controlled in a wide range, starting from 2 to more than 1000 nm in the solvent-free state.

Peng et al. [121] reported the synthesis of polymer brushes with liquid crystalline (LC) chains. A methacrylate derivative with a phenylbenzoate mesogenic side chain was synthesized. A surface-immobilized azo initiator was used to produce LC polymer brushes by polymerization of the phenylbenzoate monomer. LC brushes with thicknesses up to 200 nm in the dry state were obtained. The nematic–isotropic transition temperature of the LC brushes was 2–3° higher than that of spin-cast films made from the same polymer. The authors suggested that this difference could be due to chain stretching of the brushes and a concurrent stabilization of the nematic LC phase.

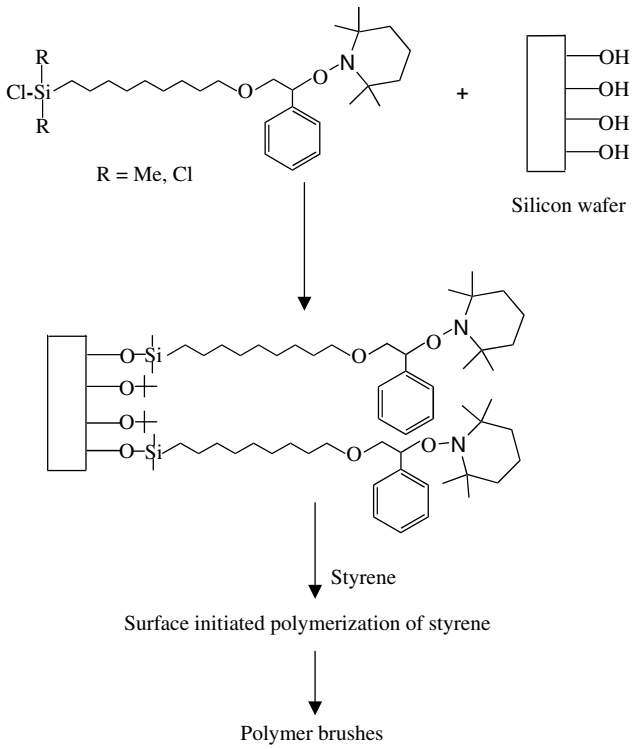

Fig. 12. Synthesis of polystyrene brushes by TEMPO-mediated radical polymerization. Reprinted with permission from Macromolecules 1999;32:1424. © 2000 American Chemical Society [126].

4.3.3. Synthesis of tethered polymer brushes by controlled radical polymerization

In order to achieve a better control of molecular weight and molecular weight distribution and synthesize novel polymer brushes like block copolymer brushes, controlled radical polymerizations including ATRP, reverse ATRP, TEMPO-mediated and iniferter radical polymerizations have been used to synthesize tethered polymer brushes on solid substrate surfaces [124–129].

In the early 1980s, Otsu et al. [130,131] reported that the polymerization of styrene and MMA in solution was living-like by using dithiocarbamate derivatives as initiators which were described as iniferters. Iniferters means that they act as initiator, transfer agent and terminator. It was also reported that photolysis of the iniferter *N*,*N*-diethyldithiocarbamate by UV irradiation yielded a reactive radical and nonreactive radical which exclusively led to termination reaction through recombination with a growing polymer chain. By use of this method, they successfully grafted PS and PMMA onto cross-linked polystyrene containing dithiocarbamate groups [127]. On the basis of Otsu's work, Nakayama and Matsuda [124] immobilized *N*,*N*-diethyldithiocarbamate groups on a cross-linked chloromethylated PS. Irradiation of this initiator-immobilized surface in the presence of a vinyl monomer such as *N*,*N*-dimethylacrylamide, *N*-[3-(dimethylamino)- propyl]acrylamide, methacrylic acid or styrene at room temperature produced tethered polymers. Since polymerization proceeded only during photoirradiation and at irradiated areas, a precise spatial control could be achieved. Recently, de Boer et al. [129] prepared polymer brushes using surface-grafted iniferter monolayers.

ATRP is a newly developed controlled radical polymerization [132]. It has attracted considerable attention due to its control of molecular weight, molecular weight distribution and synthesis of block copolymers. Ejaz et al. [125] and Husseman, et al. [126] applied ATRP in the synthesis of tethered polymer brushes on silicon wafers and achieved great success. Ejaz et al. immobilized the ATRP initiator 2-(4-chlorosulfonylphenyl)ethyltrimethoxysilane onto a silicate substrate by Langmuir–Blodgett techniques. Surface initiated polymerization from the immobilized initiators in the presence of MMA under suitable conditions produced PMMA brushes with high grafting density. The molecular weight and molecular weight distribution were controlled by addition of a predetermined amount of free initiator in the polymerization systems. Hussemann et al. prepared SAMs of 5′-trichlorosilylpentyl-2-bromo-2-methylpropionate on silicate substrates. The α-bromoester is a good initiator for ATRP. They have successfully synthesized PMMA brushes by the polymerization of MMA initiated from the SAMs. It has also been reported that tethered polyacrylamide has been obtained from surface initiated ATRP of acrylamide on a porous silica gel surface [127]. Recently, Matyjaszewski et al. [133] reported a detailed study of polymer brush synthesis using ATRP.

Alkoxyamine initiators are another class of initiators for controlled radical polymerization. Based on a recent report of Hawker and coworkers [134], this method has been extended from polymerization of styrene to other monomers such as acrylates, acrylamides and acrylonitrile. They also immobilized this type of initiator onto silicate surfaces by SAMs (see Fig. 12) [126]. However, the initial attempt to control polymer growth from the surface bound alkoxyamine initiator was unsuccessful due to the extremely low initiator concentration. Adding free alkoxyamine initiator in the polymerization solution successfully controlled the polymerization. It was found that the thickness of polymer brushes increased linearly with conversion and the variation of the thickness of PS brushes with molecular weight was also linear. The cross-sectional area per chain was ca. 2 nm^2. The PS chains were cleaved off the substrate. Analysis by GPC indicated that the polydispersity was 1.14, which was very close to that of the polymer obtained in bulk polymerization. Weimer et al. [135] attached a TEMPO initiator to a mica-type layered silicate via ion exchange. In situ living free radical polymerization resulted in a dispersed nanocomposite.

4.3.4. Synthesis of tethered polymer brushes by carbocationic polymerization

In the early 1980s, Vidal et al. [136,137] used carbocationic polymerization to graft polyisobutylene on a silica surface. They modified the silica gel surface with 2-(chloromethylphenyl)ethyldimethylchlorosilane. The immobilized initiators interacted with diethylaluminum chloride to produce carbocationic species which initiated the polymerization of isobutylene. High grafting rates, grafting ratios and grafting efficiencies were obtained in experiments using C_2H_5Cl as solvent, with Et_2AlCl/surface Cl = 20 at −50°C for 30 min.

Recently Jordan and Ulman [138] synthesized tethered poly(*N*-propionylethylenimine) on gold surfaces. They first formed a hydroxy-terminated SAM on gold surfaces and then exposed the monolayer to a constant stream of trifluoromethanesulfonic anhydride vapor for about 1 h. The conversion of hydroxy groups to triflate functional groups occurred overnight in a sealed reaction vessel. The surface initiated cationic polymerization of 2-ethyl-2-oxazoline was allowed to proceed for 7 days under reflux. Ellipsometry measurements indicated that a 10 nm polymer brush was obtained. The polymer brushes were characterized by contact angle measurements and FTIR spectroscopy. The external reflection FTIR spectrum of this polymer brush was very similar to that of a bulk polymer. The polymer chains were functionalized with an alkyl moiety by means of a termination reaction with *N*,*N*-dioctadecylamine.

However the conversion of the hydroxy group to the triflate group was not well characterized and the initiation efficiency was not determined.

Zhao and Brittain [139] reported the synthesis of PS brushes via carbocationic polymerization. 2-(4-trichlorosilylphenyl)-2-methoxy-d_3-propane was immobilized on a silicate substrate; $TiCl_4$-catalyzed polymerization of styrene produced PS brushes. FTIR-ATR was used to monitor initiator efficiency by monitoring the diminution of the υ(C-D) absorption. An initiation efficiency of 7% was observed for the formation of a 34 nm thick brush; additional initiator was consumed in a second, sequential styrene polymerization. Factors that influenced brush thickness included solvent polarity, Lewis base additives, and $TiCl_4$ concentration.

4.3.5. Synthesis of tethered polymer brushes by anionic polymerization

Living anionic polymerization is a good technique to prepare tailored polymers. Jordan et al. [140] used anionic polymerization to synthesize polystyrene brushes on gold substrates. The SAM of 4′-bromo-4-mercaptobiphenyl was prepared on a gold substrate and then reacted with *s*-BuLi to form a monolayer of biphenyllithium. Tethered polystyrene brushes with a dry thickness of 18 nm were obtained from surface initiated anionic polymerization. Based on the results from in situ swelling experiments which was monitored by ellipsometry, a grafting density of 3.2–3.6 nm^2/chain and a degree of polymerization of 382 were calculated with the use of mean-field theory.

Using a similar strategy, Ingall et al. [141] formed a SAM of 3-bromopropylsilane monolayer on the substrate. This monolayer was then lithiated with lithium di-*tert*-butylbiphenyl and subsequent addition of monomer to the system initiated the anionic polymerization. A tethered poly(acrylonitrile) film with a thickness up to 245 nm was obtained if the polymerization was allowed to proceed for 8 days.

4.3.6. Synthesis of polymer brushes by other polymerization methods

Ring-opening metathesis polymerization (ROMP), group transfer polymerization (GTP) and other polymerization methods have also been employed in the synthesis of tethered polymer brushes. Herrman and coworkers [142] immobilized a tris(neopentyl)nitridomolybdenum metathesis catalyst onto silica and performed ROMP of norbornene. Weck et al. [143] formed a norbonene-terminated SAM on the substrate and then generated initiating species by exposing the substrate to a CH_2Cl_2 solution of a ruthenium-based ROMP initiator. Surface initiated polymerization produced polynorbonene brushes on the surface. Buchmeiser and coworkers [144] used ROMP to prepare polymer brushes composed of norbornene-based L-valine- and L-phenylalanine-containing chiral monomers. PS-(divinyl benzene)-based supports were derivatized with a norbornene substrate. Treatment of the support with an Mo or Ru metathesis initiator followed by exposure to monomer produced the target polymer brushes which were studied for chiral HPLC separations.

Through a multistep process, Hertler [145] immobilized silyl ketene acetals onto cross-linked polystyrene beads. Grafted PMMA and polyacrylonitrile on the cross-linked PS beads were obtained by surface initiated GTP at -50°C in THF in the presence of an anionic catalyst. Huber et al. [146] stabilized nanometer gold particles by alkanethiols in which hydroxy groups were capable of coordinating titanium (IV). The resulting titanium (IV) alkoxide species catalyzed polymerization of *n*-hexyl isocyanate under very mild conditions. Poly(*n*-hexyl isocyanate) covalently attached to the gold nanoparticles was obtained.

Grafted polypeptide films on solid substrate surfaces have attracted considerable attention in recent years [15,147–152]. Heise et al. [150] reported the polymerization of *N*-carboxyanhydrides initiated

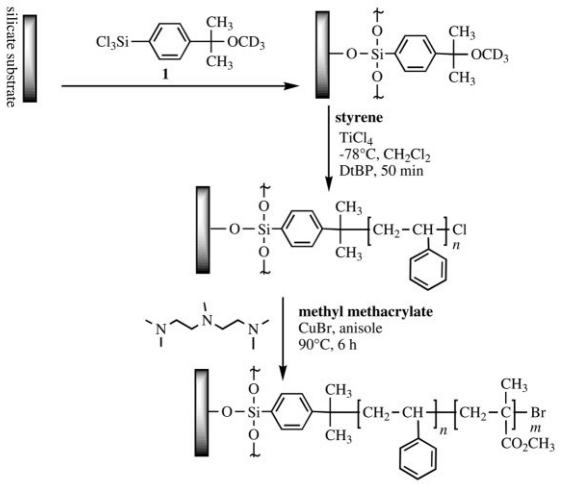

Fig. 13. Synthesis of tethered PS-*b*-PMMA block copolymer brush.

from amino-terminated SAMs on silicon substrates. In 1993, Whitesell and Chang [147] reported polyalanine chains grown from an evaporated gold surface. The polymerization of a cyclic monomer initiated from a surface bound primary amine was carried out and the resulting polymer was estimated to have an average degree of polymerization of 600 with a large polydispersity. Chang and Frank [151] reported a novel dry process for surface deposition-polymerization of vapor phase α-amino acid *N*-carboxy anhydride from a surface immobilized initiator layer. The silicon surface was modified with the coupling agent, (3-aminopropyl)triethoxysilane, in which the primary amine was a good initiator for ring-opening polymerization of γ-benzyl-L-glutamate *N*-carboxy anhydride. A film with thickness of 40 nm was obtained by this method.

5. Synthesis of tethered diblock copolymer brushes

Little work has been devoted to the synthesis of diblock copolymer brushes. Hussemann et al. [126] reported the synthesis of block copolymer brushes on silicate substrates using surface initiated TEMPO mediated radical polymerization. However, the copolymer brushes were not diblock copolymer brushes in a strict definition. The first block was PS, while the second block was a 1:1 random copolymer of styrene/MMA.

Zhao and Brittain [28,153,154] reported the synthesis of PS-*b*-poly(acrylate) tethered diblock copolymer brushes. The properties of these diblock brushes were studied using water contact angles, ellipsometry, X-ray photoelectron spectroscopy (XPS), FTIR spectroscopy and AFM. Fig. 13 shows the synthesis of PS-*b*-poly(methyl methacrylate) [28]. The synthetic route involved the following sequence: (1) surface immobilization of 2-methoxy-d_3-2-(4-trichlorosilylphenyl)propane (1) onto a silicate substrate; (2) carbocationic polymerization of styrene; and (3) ATRP of MMA. The reaction of MMA with the polystyrene film presumably involved chloro-terminated polystyrene chains as initiators. The samples of tethered diblock polymers exhibited reversible surface changes in response to solvent

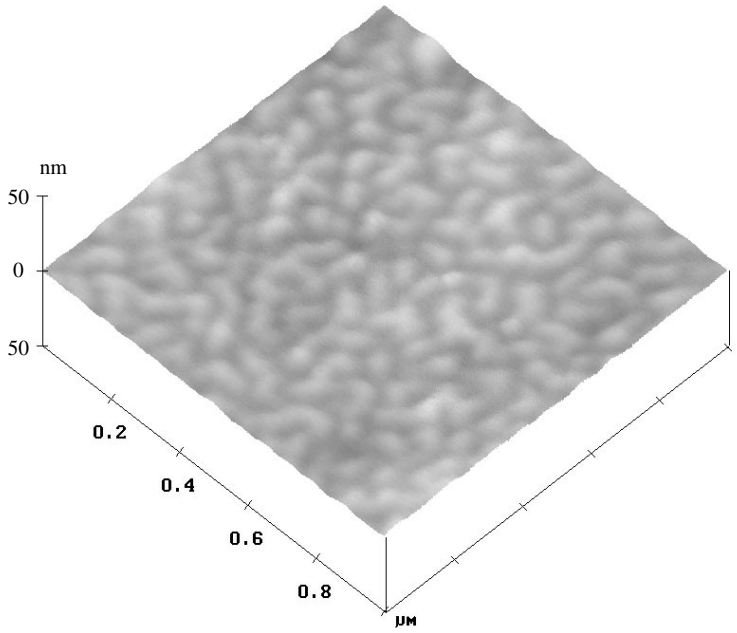

Fig. 14. AFM image of a PS-b-PMMA brush with 23 PS and 14 nm PMMA after treatment with CH_2Cl_2 at room temperature for 30 min. Reprinted with permission from J Am Chem Soc 2000;122:2407. © 2000 American Chemical Society [153].

treatment. For a sample with a 26 nm polystyrene layer and a 9 nm PMMA layer, the advancing water contact angle increased from 75 (characteristic of PMMA) to 99° (characteristic of polystyrene) after treatment with cyclohexane; subsequent treatment with CH_2Cl_2 returned the contact angle to the original value of 75°. This contact angle change was attributed to reversible changes in the chemical composition at the polymer–air interface. XPS analysis indicated large compositional changes after treatment with CH_2Cl_2 and cyclohexane which are consistent with the contact angle observations.

For a sample with 23 nm PS layer and 14 nm PMMA layer, AFM was used to study surface morphological changes [153]. It was found the surface is relatively smooth with a roughness of 0.77 nm after CH_2Cl_2 treatment (see Fig. 14); treatment with cyclohexane at 35°C for 1 h increased the surface roughness to 1.79 nm and created an irregular worm-like structure on the surface. A nanopattern was formed if mixed solvents of CH_2Cl_2 and cyclohexane were used and the composition was gradually changed from CH_2Cl_2 to cyclohexane (see Fig. 15). The advancing water contact angle of this surface was 120°.

Zhao and Brittain [154] have also prepared diblocks composed of PS and poly(methyl acrylate) (PMA) and poly(*N*,*N*-dimethylaminoethyl methacrylate). These tethered diblocks also display reversible changes in contact angles in response to selective solvent treatment. AFM study of the PS-*b*-PMA brushes revealed a different morphology after treatment with CH_2Cl_2, which is likely due to the higher Flory–Huggins interaction parameter between PS and PMA. Like tethered PS-*b*-PMMA, nanopatterns appeared if a mixed solvent of CH_2Cl_2 and cyclohexane was used and the composition was gradually

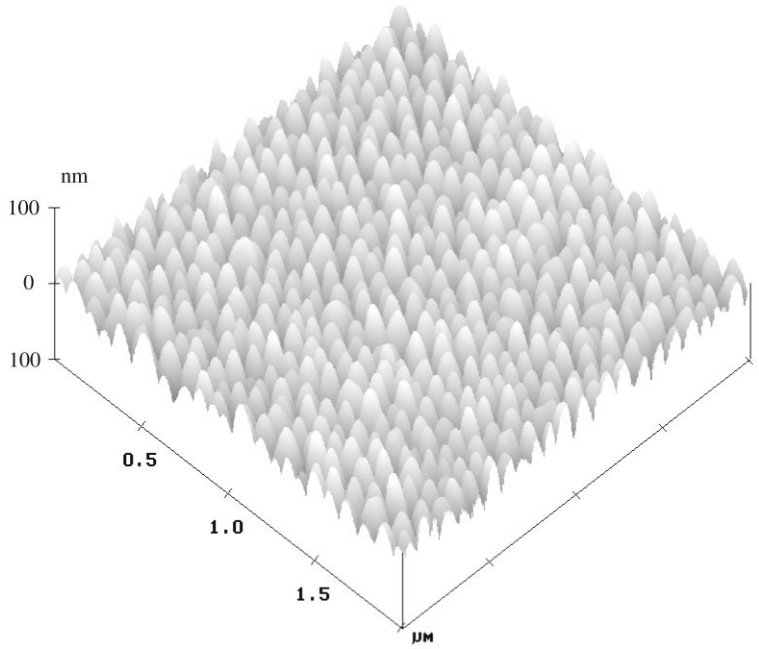

Fig. 15. Nanopattern formed from a PS-*b*-PMMA brush with 23 nm PS and 14 nm PMMA. Reprinted with permission from J Am Chem Soc 2000;122:2407. © 2000 American Chemical Society [153].

changed from CH_2Cl_2 to cyclohexane. The nanopattern scale was dependent on the thickness of the tethered diblock brushes.

Sedjo et al. [128] synthesized tethered PS-*b*-PMMA brushes using reverse ATRP. This method used a surface-immobilized azo initiator; polymerization of styrene with $CuBr_2$ under ATRP conditions produced a PS film that was capable of initiating MMA polymerization. These diblock copolymer brushes displayed reversible changes in contact angles analogous to the PS-*b*-PMMA diblock brushes prepared by carbocationic polymerization and ATRP.

Matyjaszewski et al. [133] reported the synthesis of poly(styrene-*b*-*tert*-butyl acrylate) brushes from SAMs by ATRP. Hydrolysis of these diblock copolymer brushes yielded poly(styrene-*b*-acrylic acid) brushes.

6. Synthesis of patterned polymer brushes

Patterned polymer brushes could be obtained by traditional photolithography or chemical amplification of patterned SAMs. Rühe and coworkers [122] explored preparation of patterned, covalently tethered polymer brushes by photolithography using an appropriate mask and deep or near UV irradiation before, during and after polymer formation. Three approaches were tried. First, surface reactions were carried out to remove tethered polymer chains from selected areas. The second approach used light irradiation to decompose immobilized azo initiators in selected areas followed by polymer formation through thermally induced radical polymerization in the unirradiated areas. The third technique was

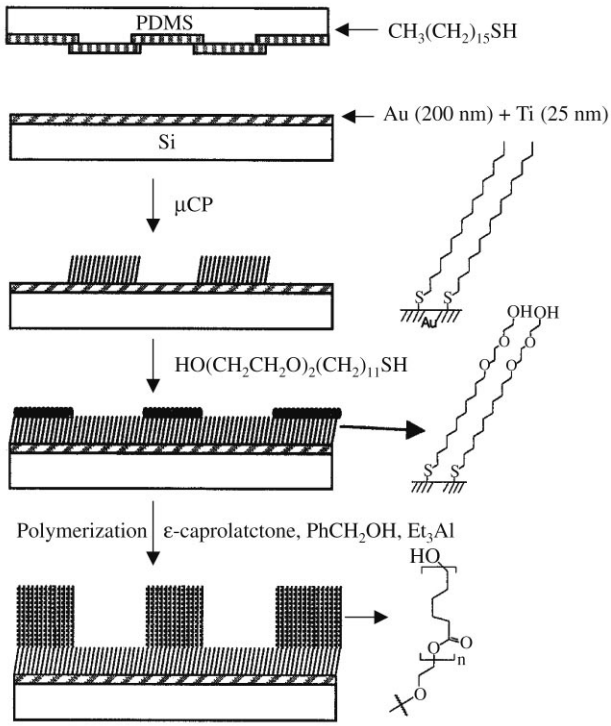

Fig. 16. Strategy for amplification of a patterned SAM prepared by microcontact printing into a patterned polymer brush. Reprinted with permission from Angew Chem Int Ed Engl 1999;38:647. © 2000 Wiley-VCH [158].

photoactivation of an initiator through a mask leading to photopolymerization in selected areas. All three approaches allowed preparation of patterned, covalently tethered polymer brushes with a high spatial resolution. Using photolithography, Chen et al. [155] obtained micropatterned, immobilized poly(acrylic acid) on a polystyrene film. Hawker and workers [156] used TEMPO-mediated radical polymerization to prepare a poly(*tert*-butyl acrylate) brush on a silicate substrate. A polystyrene film containing bis(*tert*-butylphenyl)iodonium triflate was spin-cast onto the polymer brush followed by exposure of the surface to UV radiation through a mask. Photogenerated acid converted poly(*tert*-butyl acrylate) brushes to poly(acrylic acid) brushes. The end result was a patterned surface containing distinct areas of hydrophobic and hydrophilic brushes.

Whitesides and coworkers [157] have introduced the concept of microcontact printing (μCP) to prepare patterned SAMs. This method has been extended into patterning polymer films [158–161]. Husemann et al. [158] have successfully achieved patterned, covalently tethered polymer brushes by chemical amplification from patterned SAMs with hydroxyl and methyl terminal groups. Their strategy is illustrated in Fig. 16. Di(ethylene glycol)- and methyl-terminated monolayers were patterned by microcontact printing on gold surface. Surface-initiated ring opening polymerization of ϵ-caprolactone in the presence of a free initiator such as benzyl alcohol catalyzed by triethylaluminum under suitable conditions produced tethered polymer brushes in the hydroxyl functionalized areas. It was found that the thickness of poly(ϵ-caprolactone) varied

linearly with the M_n of the free polymer formed in solution from the added initiator. Shah et al. [162] used ATRP to amplify initiator monolayers prepared by microcontact printing on gold surfaces.

Whitesides and coworkers [163] reported patterned polymer growth on silicon surfaces using microcontact printing and surface-initiated polymerization. Microcontact printing was used to prepare a patterned SAM composed of octadecyltrichlorosilane and norbornenyl tirchlorosilane. Exposure of the surface to an Ru metathesis catalyst followed by surface-initiated ROMP of norbornene produced patterned polymer brushes. The patterned polymer films were successfully used as reactive ion etching resists.

References

[1] Milner ST. Science 1991;251:905.
[2] Halperin A, Tirrell M, Lodge TP. Adv Polym Sci 1992;100:31.
[3] Szleofer I, Carignano MA. Adv Chem Phys 1996;94:165.
[4] Van der Waarden M. J Colloid Sci 1950;5:317.
[5] Van der Waarden M. J Colloid Sci 1951;6:443.
[6] Mackor EL. J Colloid Sci 1951;6:492.
[7] Mackor EL, van der Waals JH. J Colloid Sci 1952;7:535.
[8] Clayfield EJ, Lumb EC. J Colloid Interface Sci 1966;22:269.
[9] Clayfield EJ, Lumb EC. J Colloid Interface Sci 1966;22:285.
[10] Raphaël E, de Gennes PG. J Phys Chem 1992;96:4002.
[11] Ji H, de Gennes PG. Macromolecules 1993;26:520.
[12] Amiji M, Park KJ. Biomater Sci Polym Ed 1993;4:217.
[13] Van Zanten JH. Macromolecules 1994;27:6796.
[14] Joanny J-F. Langmuir 1992;8:989.
[15] Takei YG, Aoki T, Sanui K, Ogata N, Sakurai Y, Okano T. Macromolecules 1994;27:6163.
[16] Ito Y, Ochiai Y, Park YS, Imanishi Y. J Am Chem Soc 1997;119:1619.
[17] Ito Y, Park YS, Imanishi Y. J Am Chem Soc 1997;119:2739.
[18] Ito Y, Nishi SW, Park YS, Imanishi Y. Macromolecules 1997;30:5856.
[19] Velten U, Shelden RA, Caseri WR, Suter UW, Li YZ. Macromolecules 1999;32:3590.
[20] Velten U, Tossati S, Shelden RA, Caseri WR, Suter UW, Hermann R, Muller M. Langmuir 1999;15:6940.
[21] Niu QJ, Fréchet JMJ. Angew Chem, Int Ed Engl 1998;37:667.
[22] Singhvi R, Kumar A, Lopez GP, Stephanopoulos GN, Wang DIC, Whitesides GM, Ingber DE. Science 1996;273:892.
[23] Chen CS, Mrksich M, Huang S, Whitesides GM, Ingber DE. Science 1997;276:1425.
[24] Aksay A, Trau M, Manne S, Honma I, Yao N, Zhou L, Fenter P, Eisenberger PM, Gruner SM. Science 1996; 273:892.
[25] Balazs AC, Singh C, Zhulina E, Gersappe D, Pickett G. MRS Bull 1997;16:1.
[26] Soga K, Zuckermann MJ, Guo H. Macromolecules 1996;29:1998.
[27] Mansky P, Liu Y, Huang E, Russell TP, Hawker CJ. Science 1997;275:1458.
[28] Zhao B, Brittain WJ. J Am Chem Soc 1999;121:3557.
[29] Alexander SJ. J Phys (Paris) 1977;38:977.
[30] de Gennes PG. J Phys (Paris) 1976;37:1443.
[31] de Gennes PG. Macromolecules 1980;13:1069.
[32] Cantor R. Macromolecules 1981;14:1186.
[33] Flory PJ. Principles of polymer chemistry. Ithaca, NY: Cornell University Press, 1981.
[34] Halperin A. J Phys (Paris) 1988;49:547.
[35] Semenov AN. Sov Phys JETP 1975;61:733.
[36] Milner ST, Whitten TA. J Phys (Paris) 1988;49:1951.

[37] Milner ST, Whitten TA, Cates ME. Macromolecules 1989;22:1951.
[38] Zhulina EB, Borisov OV, Priamitsyn VA. J Colloid Interface Sci 1990;137:495.
[39] Allain C, Ausserr D, Rondelez F. Phys Rev Lett 1981;49:1694.
[40] Sauer DB, Yu H, Kim MW. Langmuir 1989;5:278.
[41] Kawaguchi M, Kawarabayashi M, Nagata N, Kato T, Yoshioka A, Takahashi A. Macromolecules 1988;21:1059.
[42] Munch MR, Gast AP. Macromolecules 1990;23:2313.
[43] Munch MR, Gast AP. J Chem Soc Faraday Trans 1990;86:1341.
[44] Cosgrove T, Ryan K. Langmuir 1990;6:1361.
[45] Cosgrove T, Heath TG, Ryan K, Crowley TL. Macromolecules 1987;20:1361.
[46] Parsonage E, Tirrell M, Watanabe H, Nuzzo R. Macromolecules 1987;24:1987.
[47] Patel S, Hadziioannon G, Tirrell M. Proc Natl Acad Sci USA 1987;84:4725.
[48] Auroy P, Auvray L, Leger L. Phys Rev Lett 1991;66:719.
[49] Murat M, Grest GS. Phys Rev Lett 1989;63:1074.
[50] Murat M, Grest GS. Macromolecules 1991;22:4054.
[51] Murat M, Grest GS. Macromolecules 1993;24:704.
[52] Kuznetsov DV, Chen ZY. J Chem Phys 1998;109:7017.
[53] Amoskov VM, Birshtein TM, Pryamitsyn VA. Macromolecules 1996;29:7240.
[54] Amoskov VM, Birshtein TM, Pryamitsyn VA. Macromolecules 1998;31:3720.
[55] Birshtein TM, Amoskov VM, Mercurieva AA, Pryamitsyn VA. Macromol Symp 1997;113:151.
[56] Wijmans CM, Leermaker FAM, Fleer GJ. J Chem Phys 1994;101:8214.
[57] Pickett GT, Witten TA. Macromolecules 1992;25:4569.
[58] Mercurieva AA, Birshtein TM, Pryamitsyn VA, Polotskij A. Macromol Chem Theory Simul 1996;5:215.
[59] Khokhlov AR, Semenov AN. Physica A 1981;109:546.
[60] Marko JF, Witten TA. Phys Rev Lett 1991;66:1541.
[61] Zhulina EB, Borisov OV, Birshtein TM. J Phys II 1992;2:63.
[62] Borisov OV, Zhulina EB, Birshtein TM. Macromolecules 1994;27:4795.
[63] Zhulina EB, Birshtein TM, Borisov OV. Macromolecules 1995;28:1491.
[64] Pryamitsyn VA, Leermakers FAM, Zhulina EB. Macromolecules 1997;30:584.
[65] Israels R, Leermakers FAM, Fleer GJ, Zhulina EB. Macromolecules 1994;27:3249.
[66] Pincus P. Macromolecules 1991;24:2912.
[67] Marko JF, Witten TA. Macromolecules 1992;25:296.
[68] Brown G, Chakrabarti A, Marko JF. Europhys Lett 1995;25:239.
[69] Dong H. J Phys II Fr 1993;3:999.
[70] Lai P-Y. J Chem Phys 1994;100:3351.
[71] Dong H, Marko JF, Witten TA. Macromolecules 1994;27:6428.
[72] Zhulina EB, Singh C, Balazs AC. Macromolecules 1996;29:6338.
[73] Zhulina EB, Balazs AC. Macromolecules 1996;29:2667.
[74] Zhulina EB, Singh C, Balazs AC. Macromolecules 1996;29:8254.
[75] Singh C, Balazs AC. Macromolecules 1996;29:8904.
[76] Gersappe G, Fasolka M, Israels R, Balazs AC. Macromolecules 1995;28:4753.
[77] Chern S-S, Zhulina EB, Pickett GT, Balazs AC. J Chem Phys 1998;108:5981.
[78] Gersappe G, Fasolka M, Balazs AC, Jacobson SH. J Chem Phys 1994;100:1970.
[79] Li W, Balazs AC. Mol Simul 1994;13:257.
[80] Bug ALR, Cates ME, Safran SA, Witten TA. J Chem Phys 1987;87:1824.
[81] Marra J, Hair ML. Colloids Surf 1989;34:215.
[82] Guzonas D, Boils D, Hair ML. Macromolecules 1991;24:3383.
[83] Fytas G, Anastasiadis SH, Seghrouchni R, Vlassopoulos D, Li J, Factor BJ, Theobald W, Toprakcioglu C. Science 1996;274:2041.
[84] Field JB, Toprakcioglu C, Ball RC, Stanley HB, Dai L, Barford W, Penfold J, Smith G, Hamilton W. Macromolecules 1992;25:434.
[85] Motschmann H, Stamm M, Toprakcioglu C. Macromolecules 1991;24:3681.
[86] Kelley TW, Schorr PA, Johnson KD, Tirrell M, Frisbie CD. Macromolecules 1998;31:4297.

[87] Fleer GJ, Cohen-Stuart MA, Scheutjens JMH, Cosgrove T, Vincent B. Polymers at interfaces. London: Chapman and Hall, 1993.
[88] Zerushalmi-Royen R, Klein J, Fetters L. Science 1994;263:793.
[89] Reiter G. Europhys Lett 1996;33:29.
[90] Koutsos V, Van der Vegte EM, Hadziioannou G. Macromolecules 1999;32:1233.
[91] Koutsos V, Van der Vegte EM, Pelletier E, Stamouli A, Hadziioannou G. Macromolecules 1997;30:4719.
[92] Bergbreiter DE, Franchina JG, Kabza K. Macromolecules 1999;32:4993.
[93] Yang X, Shi J, Johnson S, Swanson B. Langmuir 1998;14:1505.
[94] Ebata K, Furukawa K, Matsumoto N. J Am Chem Soc 1998;120:7367.
[95] Wells M, Crooks RM. J Am Chem Soc 1996;118:3988.
[96] Tran Y, Auroy P, Lee LT. Macromolecules 1999;32:8952.
[97] Prucker O, Naumann CA, Rühe J, Knoll W, Frank CW. J Am Chem Soc 1999;121:8766.
[98] Ito Y, Park YS, Imanishi Y. Macromol Rapid Commun 1997;18:221.
[99] Park YS, Ito Y, Imanishi Y. Macromolecules 1998;31:2606.
[100] Yamaguchi T, Ito T, Sato T, Shinbo T, Nakao S. J Am Chem Soc 1999;121:4078.
[101] Iwata H, Hirata I, Ikada Y. Macromolecules 1998;31:3671.
[102] Suzuki M, Kishida A, Iwata H, Ikada Y. Macromolecules 1986;19:1804.
[103] Boven G, Folkersma R, Challa G, Schouten AJ. Polym Commun 1991;32:50.
[104] Hamann R, Laible R. Angew Makromol Chem 1973;48:97.
[105] Boven G, Oosterling MCLM, Challa G, Schouten AJ. Polymer 1991;31:2377.
[106] Sugawara T, Matsuda T. Macromolecules 1994;27:7809.
[107] Guo X, Weiss A, Ballauff M. Macromolecules 1999;32:6043.
[108] Minko S, Gafijchuk G, Sidorenko A, Voronov S. Macromolecules 1999;32:4525.
[109] Minko S, Sidorenko A, Stamm M, Gafijchuk G, Senkovsky V, Voronov S. Macromolecules 1999;32:4532.
[110] Sidorenko A, Minko S, Galfijchuk G, Voronov S. Macromolecules 1999;32:4539.
[111] Minko SS, Luzinov IA, Evchuk IY, Voronov SA. Polymer 1996;37:177.
[112] Luzinov IA, Evchuk IY, Minko SS, Voronov SA. J Appl Polym Sci 1998;67:299.
[113] Luzinov IA, Voronov A, Minko SS, Kraus R, Wilke W, Zhuk A. J Appl Polym Sci 1996;61:1101.
[114] Luzinov IA, Minko SS, Senkovsky V, Voronov A, Hild S, Marti O, Wilke W. Macromolecules 1998;31:3945.
[115] Tsubokawa N, Kogure A, Maruyama K, Sone Y, Shimomura M. Polym J 1990;22:827.
[116] Sidorenko A, Minko S, Schenk-Meuser K, Duschner H, Stamm M. Langmuir 1999;15:8349.
[117] Prucker O, Rühe J. Macromolecules 1998;31:592.
[118] Prucker O, Rühe J. Macromolecules 1998;31:602.
[119] Prucker O, Rühe J. Langmuir 1998;14:6893.
[120] Biesalski M, Rühe J. Macromolecules 1999;32:2309.
[121] Peng B, Johannsmann D, Rühe J. Macromolecules 1999;32:6759.
[122] Rühe J. Macromol Symp 1997;126:215.
[123] Tovar G, Paul S, Knoll W, Prucker O, Rühe J. Supramol Sci 1995;2:89.
[124] Nakayama Y, Matsuda T. Macromolecules 1996;29:8622.
[125] Ejaz M, Yamamoto S, Ohno K, Tsujii Y, Fukuda T. Macromolecules 1998;31:5934.
[126] Husseman M, Malmstrom EE, McNamara M, Mate M, Mecerreyes O, Benoit DG, Hedrick JL, Mansky P, Huang E, Russell TP, Hawker CJ. Macromolecules 1999;32:1424.
[127] Huang X, Wirth MJ. Macromolecules 1999;32:1094.
[128] Sedjo RA, Mirous BK, Brittain WJ. Macromolecules 2000;33:1492.
[129] de Boer B, Simon HK, Werts MPL, van der Vegte EW, Hadziioannou I. Macromolecules 2000;33:349.
[130] Otsu T, Yoshida M. Makromol Chem Rapid Commun 1982;3:127.
[131] Otsu T, Yoshida M, Tazaki T. Makromol Chem Rapid Commun 1982;3:133.
[132] Patten TE, Xia J, Abernathy T, Matyjaszewski K. Science 1996;272:866.
[133] Matyjaszewski K, Miller PJ, Shukla N, Immaraporn B, Gelman A, Luokala BB, Siclovan TM, Lickelbick G, Vallant T, Hoffmann H, Pakula T. Macromolecules 1999;32:8716.
[134] Benoit D, Chaplinski V, Hawker CJ. J Am Chem Soc 1999;121:3904.
[135] Weimer MW, Chen H, Giannelis EP, Sogah DY. J Am Chem Soc 1999;121:1615.

[136] Vidal A, Guyot A, Kennedy JP. Polym Bull 1980;2:315.
[137] Vidal A, Guyot A, Kennedy JP. Polym Bull 1982;6:401.
[138] Jordan R, Ulman A. J Am Chem Soc 1998;120:243.
[139] Zhao B, Brittain WJ. Macromolecules 2000;33:342.
[140] Jordan R, Ulman A, Kang JF, Rafailovich MH, Sokolov J. J Am Chem Soc 1999;121:1016.
[141] Ingall MDK, Honeyman CH, Mercure JV, Bianconi PA, Kunz RR. J Am Chem Soc 1999;121:3607.
[142] Herrmann WA, Stumpf AW, Priermeier T, Bogdanovic S, Dufaud V, Basset J-M. Angew Chem, Int Ed Engl 1996;35:2803.
[143] Weck M, Jackiw JJ, Rossi RR, Weiss PS, Grubbs RH. J Am Chem Soc 1999;121:4088.
[144] Buchmeiser MR, Sinner F, Mupa M, Wurst K. Macromolecules 2000;33:32.
[145] Hertler WR, Sogah DY, Boettcher FP. Macromolecules 1990;23:1264.
[146] Huber DL, Gonsalves KE, Carlson G, Seery TAP. In: Lohse DJ, Russell TP, Sperling LH, editors. Interfacial aspects of multicomponent polymer materials, New York: Plenum Press, 1997. p. 107.
[147] Chang Y-C, Frank CW. Langmuir 1996;12:5824.
[148] Machida S, Urano TI, Sano K, Kawata Y, Sunohara K, Sasaki H, Yoshiki M, Mori Y. Langmuir 1995;11:4838.
[149] Wieringa RH, Schouten AJ. Macromolecules 1996;29:3032.
[150] Heise A, Menzel H, Yim H, Foster MD, Wieringa RH, Schouten AJ, Erb V, Stamm M. Langmuir 1997;13:723.
[151] Chang Y-C, Frank CW. Langmuir 1998;14:326.
[152] Whitesell JK, Chang HK. Science 1993;261:73.
[153] Zhao B, Brittain WJ, Zhou W, Cheng SZD. J Am Chem Soc 2000;122;2407.
[154] Zhao B, Brittain WJ. Submitted for publication.
[155] Chen G, Ito Y, Imanishi Y. Macromolecules 1997;30(30):7001.
[156] Husemann M, Morrison M, Benoit D, Frommer J, Mate CM, Hinsberg WD, Hedrick JL, Hawker CJ. J Am Chem Soc 2000;122;1844.
[157] Xia Y, Whitesides GM. Angew Chem, Int Ed Engl 1998;37:550.
[158] Huesmann M, Mercerreyes D, Hawker CJ, Hedrick JL, Shah R, Abbott NL. Angew Chem Int Ed Engl 1999;38:647.
[159] Böltau M, Walheim S, Mlynek J, Krausch G, Steiner U. Nature 1998;391:877.
[160] Karim A, Douglas JF, Lee BP, Glotzer SC, Rogers JA, Jackman RJ, Amis EJ, Whitesides GM. Phys Rev E 1998;57:R6273.
[161] Hammond PT, Whitesides GM. Macromolecules 1995;28:7569.
[162] Shah RR, Merreceyes D, Huesmann M, Rees I, Abbott NL, Hawker CJ, Hedrick JL. Macromolecules 2000;33:597.
[163] Jeon NL, Choi IS, Whitesides GM, Kim NY, Laibinis PE, Harada Y, Finnie KR, Girolami GS, Nuzzo RG. Appl Phys Lett 1999;75:4201.